LAKE AND SHORE ICE CONDITIONS ON SOUTHEASTERN LAKE MICHIGAN IN THE VICINITY OF THE DONALD C. COOK NUCLEAR PLANT: WINTER 1973-74

By

Erwin Seibel, Christopher T. Carlson
and Joseph W. Maresca, Jr.[1]

Under contract with
American Electric Power Service Corporation
Indiana and Michigan Electric Company
John C. Ayers, Project Director

Special Report No. 55
Great Lakes Research Division
The University of Michigan
Ann Arbor, Michigan
1975

[1]Present address: Stanford Research Institute, Menlo Park, Calif. 94025

TABLE OF CONTENTS

ABSTRACT

A time lapse photographic system designed to take high oblique photographs of the nearshore zone at the Donald C. Cook Nuclear Plant in southeastern Lake Michigan was used to provide a nearly continuous record of ice conditions during the 1973-74 winter season. The ice conditions have been categorized into five distinct stages: no ice, static, accretion, deterioration and break-up. These five stages of ice development were related to wind direction, wind speed, air temperature and water temperature. A typical sequence of shore ice formation through breakup was established through qualitative analysis of the photographs. The typical sequence was influenced by the complex interrelationship between the climatic variables and ice stage development. Quantitative analysis of the photographs was used to test and subsequently verify the hypothesis that the nearshore ice ridges, offshore bars, and breaker zones are coincident in location at approximately 40 and 100 meters from the water's edge. The observations reveal that large quantities of sediment are incorporated into the nearshore ice and that the nearshore ice ridges ground themselves on the nearshore bottom.

We believe that the grounded nearshore ice ridges simultaneously modify the nearshore topography and protect the shoreline and bluffline from erosion by winter storms. The degree to which the nearshore is protected or modified has not yet been established.

ACKNOWLEDGMENTS

Our appreciation is expressed to the many persons who assisted in the data collection phase of this continuing project. The technical staff of the Donald C. Cook Nuclear Plant who periodically checked the monitoring system receive a special recognition for their efforts. William L. Yocum, who initially installed and saw to the proper functioning of the camera system and who participated in many discussions on ice in the proximity of the plant, receives a special thanks. James G. Fausone labelled and logged many of the processed slides. Helen Ayers and Genevieve Farris typed the draft and final manuscripts. Theodore B. Ladewski assisted in the addition of the plot routines for the computer program. Larry R. Horning drafted some of the figures. The manuscript was reviewed by Ronald Rossmann and John C. Ayers. To all the persons involved, we express a great deal of appreciation for their parts in getting this report and its findings out.

INTRODUCTION

As part of a continuing environmental study of southeastern Lake Michigan in the vicinity of the Donald C. Cook Nuclear Plant (Fig. 1), a series of time lapse photographs were taken during the winter of 1973-1974. The high oblique photographs depicting the shore and nearshore zones north of the plant provided a nearly continuous record of ice conditions during that period (see Appendix A). This made possible the observation of shore ice formation and breakup as a function of climatological variables and nearshore dynamics.

Due to the short term or irregular nature of their observations, early observers of shore ice characteristics were usually restricted to qualitative investigations of morphology or process. Some investigations (Heap 1963; Heap and Noble 1966) were dependent upon the expertise of various shore based observers at numerous stations over a large geographical area, while others (Marshall 1966) based their studies on aerial photo reconnaissance. Such data gathered for the gross evaluation of the Great Lakes ice distributions and durations of coverage could not be used in the determination of smaller scale localized formative processes.

More recently attention has been focused on the relationship between nearshore ice and nearshore morphology (Marsh et al. 1973; Ayers and Yocum 1972) and the genesis of shore ice in response to various climatological, geomorphological and hydraulic parameters (O'Hara and Ayers 1972; Bryan and Marcus 1972). Evenson (1973) reviewed efforts by Clos-Arceduc and Sonu to model the apparent regularity of beach cusps. Evenson suggested that if a model such as that developed by Clos-Arceduc was operational in the Great Lakes it might also explain the observed regularity of blowhole cones which are frequently aligned along the lakeward edge of the ice ridge complex. Attempting to establish a sequence of processes typical of shore ice formation in their geographical area of study, O'Hara and Ayers (1972) based their conclusions on the observations of photographs supplemented by intermittent field observations. Ayers et al. (1973) initiated a time lapse photographic monitoring system into their study program to supplement aerial photography. Marsh et al. (1973) utilized seismic refraction and drilling to correlate nearshore ice structure with subsurface morphology.

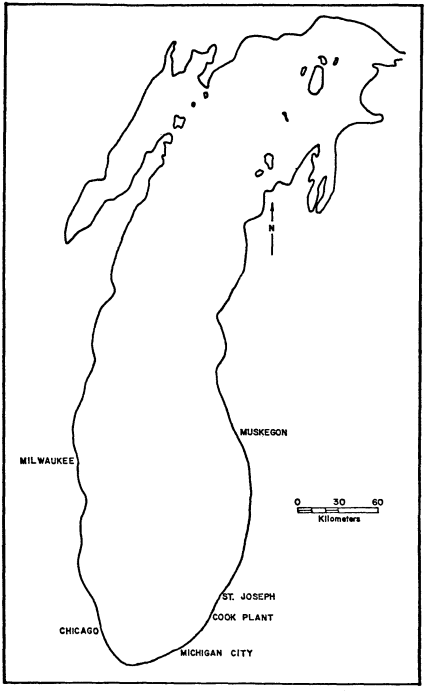

FIG. 1. Location of the Donald C. Cook Nuclear Plant.

O'Hara and Ayers (1972), Ayers et al. (1973) and Bryan and Marcus (1972) proposed that there was a correlation between the location of ice ridges and offshore sand bars. O'Hara and Ayers (1972) obtained evidence in support of this supposition through diving operations conducted on 10 March 1970 during which grounded remnant ice blocks of a deteriorated ice ridge were observed to be embedded in the bottom and thought to sit on one of the offshore bars. Ayers et al. (1973) superimposed photographs of breaking waves and ice ridges which provided additional qualitative evidence of the ice ridge - offshore bar correlation. During an aerial reconnaissance flight Bryan and Marcus (1972) observed isolated ice blocks, remnants of a deteriorating ice ridge, grounded along a continuous offshore bar.

Offshore profiles compiled by Marsh et al. (1973) revealed that a correlation does exist between offshore bars and ice ridges but they observed that within 150 meters from the Lake Superior shoreline bars existed without ice ridges located over them.

In this study, the writers investigated the correlation between breaker zone position, offshore topography and ice ridge location. Computer analysis of time lapse high oblique photographs provided a quantitative basis for discussion. Meteorological data were utilized in conjunction with the photographs to evaluate ice ridge development as a function of time, air and water temperatures and wind speed and direction.

METHODOLOGY

High oblique photographs were obtained for analysis with a Canon F-1 single reflex 35 mm camera with Canon 50 mm f 1.8 lens. The camera with Canon EE Servo Finder and special timing unit was mounted indoors facing in a NNW direction and automatically provided an average of five photographs per day from early morning to late afternoon. Since it was not possible to determine the exact time of exposure for each slide, a relative time was assigned to each photo: early am, late am, noon, early pm, and late pm. The positions of a sheet pile seawall and a range pole, evident in each photograph, were determined by standard field survey methods and were used as reference points.

The camera location permitted observation of isolated ice blocks as well as cross-sectional ice ridge profiles visible through wave breached portions of the ridge system. In each slide the horizon was evident. Reflected glare from the lake surface, ice, or window glass did not interfere with the quality of the photographs.

Slides were selected for use in the analysis instead of prints for two reasons. First, slides are less expensive to process than prints; and secondly, analysis required that the images of variables in the oblique photographs be marked on a tracing paper overlay. Slides were easily enlarged with a slide projector to minimize human error in selecting points from the image.

Representative slides or groups of slides were chosen for analysis from the sequence taken during the period from 17 January 1974 through 6 April 1974 (Appendix B). Although the camera was set up late in December 1973, photographs were not available until 17 January 1974 due to camera malfunction. As a consequence, the initial ice formation occurring late in December 1973 was not recorded. The final melt-off of isolated remnant ice blocks occurred on 6 April 1974.

Analysis of the slides was divided into three steps. First, points were marked locating the positions of variable features in the projected oblique representation, and their coordinates were determined relative to an (x, y) coordinate system with origin at the principal point of the oblique photograph. Secondly, the positions of these points were calculated for the equivalent vertical photograph with coordinate system origin at its isocenter. Finally, the real ground coordinate positions of the points were determined relative to a coordinate system with origin at the camera. The geometry basic to this method of oblique photo analysis is discussed under *Geometry of oblique photographs*.

A fixed reference system was requisite for slide-to-slide comparisons. Establishment of such a coordinate system with origin at the principal point of the projected oblique photograph necessitated the removal of the color transparency from the developer's cardboard mount and remounting on a 2.0 inch plexiglass square as suggested by Maresca (1975). Inscribed on the plastic mount were a series of lines parallel to its borders to aid in placement of

the positive. Also etched on the mount were the fiducial axes whose origin would be located at the principal point of the remounted color transparency.

The remounted slide was projected by a Kodak Ektagraphic slide projector onto a wall covered with a tracing paper overlay. The projected image of the fiducial coordinate axes, now superimposed on the projected photograph, was located on the overlay. To minimize error due to remounting, the location of the projected principal point was checked and adjusted when necessary.

The perpendicular distance was measured between two of the inscribed horizontal lines on the plastic mount, one at the top and one at the bottom of the mount. The distance between the projected image of these same two lines was measured on the screen, and these values were used in the computer program for calculation of the focal length of the projector. The positions of the reference points common to all slides were marked on the overlay and subsequently the projected positions of the variables unique in each slide were located. These variables included the horizon, breaker zones, ice ridges and interridge ice lagoons, zones of brash ice accumulations, heights of the icefoot, ice blocks, and ice ridges and the waterline when visible.

The computer program utilizes the mean still water level (MSWL) as the datum for ground coordinate calculations thus requiring that the selected data points be located at this elevation. Points defining variable positions were therefore marked on the tracing paper overlay where their intersection with the water surface was evident in the projected picture. The points marking the location of breaker zones were placed at the base of the breaking waves. Points marked along the crest of an ice ridge, above the MSWL datum, would represent only an estimate of the ridge's position (see Appendix C). Consequently, when determining ice ridge location, it was frequently necessary to use a later slide which depicted the breaching of or breakup of that ice ridge when its intersection with the water surface at midridge was visible. Points defining the outline of brash ice areas of the edges of the interridge ice lagoons were in most cases considered to be at the MSWL. The calculation of the height of a variable required two points of definition: one at the object's base where intersection with the water was apparent and the other marking its vertical extent. For the reference points, which were not located at the still water level, surveyed heights were specified in the program for

determination of their ground coordinate location.

The distance from the principal point of the oblique photograph to the apparent horizon is utilized in the program for calculation of distances on the principal plane diagram, hence, the position of a poorly defined horizon may introduce errors. The quality of the horizon was evaluated as excellent, good, fair, or poor, thus offering one possible explanation of error in poor computer output values.

The determination of the (x, y) coordinates for the points locating the positions of variables on the projected oblique photograph required a coordinate grid. Coordinate values were read to the third decimal place from a cartesian coordinate grid with a scale of twenty divisions to the inch placed under the tracing paper overlay.

The computer program converts the oblique (x, y) coordinate points to coordinates for an equivalent vertical photograph and then calculates the real ground coordinates for each ordered pair. Printer plot subroutines, called in the main program, construct a ground coordinate grid with origin at the camera. The computed ground coordinates of each data point were scaled and plotted within the grid. A unique plotted character was used for each monitored variable. Characters representing the location of each variable were positioned in linear arrays on the printer plots and were approximated by straight lines to facilitate distance measurements as described in Appendix D. The distances to all variable positions were calculated perpendicular to a baseline along the shore. The sheet pile seawall was chosen as the baseline since the waterline is subject to frequent changes in position and is usually not visible during periods of ice cover. Presently the computer program does not calculate the distances from the baseline to the various variable positions. A reference point along the baseline was established and all distance measurements were made perpendicular to the baseline from that point. A normal to the baseline was constructed of sufficient length to intersect the lines defining the variable positions. This normal formed the hypothenuse of a right triangle. Determination of the x and y components of the baseline normal and application of the plotting scale factor and the Pythagorean Theorem yielded distances to the variable's location. This technique was used to calculate the distances from the baseline to all monitored variables.

GEOMETRY OF OBLIQUE PHOTOGRAPHS

The analysis of an oblique representation can be obtained in any standard reference or text (American Society of Photogrammetry 1966), but is presented here briefly so that the correction for the projection of the image through a slide projector can be included. The geometry of the principal plane diagram (Olson 1973) (Fig. 2) was used to derive the fundamental equations required to solve the oblique photograph problem. The distance, PT, is measured on the screen from the apparent horizon to the principal point of the photograph. Since this distance is projected onto a screen from a slide projector, the image distance must be corrected for the focal length of the slide projector. A constant, C, is used to make this correction. The constant, C, is defined as

$$C = I/O \tag{1}$$

where I is the image distance and O is the object distance. The image distance, I, is calculated from the lens maker's formula

$$I = O \times f_{proj} \; / \; O - f_{proj} \tag{2}$$

where f_{proj} is the focal length of the projector. The distances on the principal plane positive can now be defined. The angle of depression, θ', is defined as

$$\tan \theta' = PT \; / \; f_{cam} \tag{3}$$

where

$$PT = PT_{screen} \times C \tag{4}$$

and f_{cam} is the focal length of the camera. The distance PT and the angle θ' was calculated to the apparent horizon. A small correction can be made to determine θ' to the true horizon by adding

$$\Delta\theta = 0.98 \sqrt{H} \tag{5}$$

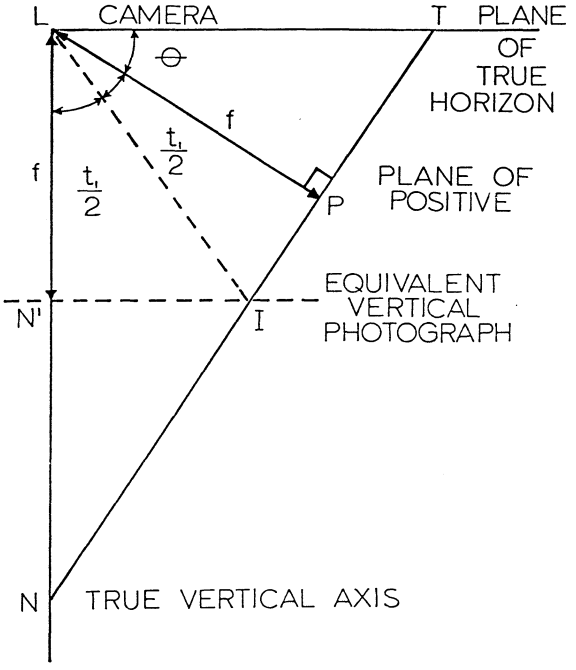

FIG. 2. Principal plane diagram.

in minutes to θ' where H is the difference in elevation between the water surface and the camera elevation. Since $\theta = \theta' + \Delta\theta$, the distance PT must be re-calculated. The geometry of the principal plane diagram (Fig. 2) may be used to derive the distance PI using

$$PI = (\tan t/2) \times f_{cam} \tag{6}$$

where t equals 90 - θ. The remaining distances in the principal plane diagram are given in equations 7, 8, and 9.

$$PN = f_{cam} \times (\tan t) \tag{7}$$

$$TI = PT + PI \tag{8}$$

$$TN = PT + PN \tag{9}$$

Using this information all points in the oblique representation can be rotated into an equivalent vertical photograph and finally real ground distances were obtained.

Individual ordered pairs, (X_{scrn}, Y_{scrn}), are picked off the oblique photographic projection on the screen relative to a rectangular coordinate system with an origin at the principal point. The coordinates, $(X_{v.p.}, Y_{v.p.})$ of the equivalent vertical photographs are calculated as

$$X_{v.p.} = X_{scrn} \times C \times (TI \,/\, (TI - K)) \tag{10}$$

$$Y_{v.p.} = K \times (TI \,/\, (TI - K)) \tag{11}$$

where

$$K = (Y_{scrn} \times C) + PI \tag{12}$$

The real ground coordinates, (X_{grd}, Y_{grd}), can be calculated from a simple proportion between the equivalent vertical photograph and the ground relative to a rectangular coordinate with the origin at the camera. The (X_{grd}, Y_{grd}) is calculated as

$$X_{grd} = H \times X_{v.p.} / f_{cam} \quad (13)$$

$$Y_{grd} = H \times (PI + Y_{v.p.}) / f_{cam} \quad (14)$$

The fundamental assumption basic to the analysis is that all points lie within the datum plane. If a point lies outside the datum, as for example a point on the beach, then a different elevation, H, must be used.

Vertical elevations or vertical heights were calculated from the formula

$$h = H \times \frac{d'}{r'} \times \frac{TN}{TS} \quad (15)$$

where d' is the height of the object on the screen, r' is the distance from the principal point to the top of the object in the oblique view, TN is the distance from point T to point N, and TS is the distance from the point T to the point S which is the base of the object.

Using the above formulae, a comprehensive computer program, ICESTUDY (Appendix E), was written to convert from the oblique to the real ground distances. The output was produced in both tabular and graphical format. The breaker zone and ice ridge locations were calculated as well as the position of the wave runup. The height of the ice ridges was calculated when visible in the photo and the area of zones of accumulated brash ice was determined.

DISCUSSION AND RESULTS

TERMINOLOGY

The terminology used in this report is that of O'Hara and Ayers (1972) and is consistent with that recommended by Kivisild (1970). The initial stage of lake ice development is the formation of a frozen beach. This is usually followed by the buildup of a small ridge or icefoot at or near the water's edge (Fig. 3a). The icefoot is the result of spray produced by waves lapping against the frozen beach face and the accumulation of brash ice fragments. Subsequent to the icefoot development is the formation of a tabular ice lagoon which terminates at the first ice ridge (Fig. 3b). Numerous, small, irregularly spaced undulations may be observed on the ice lagoon and are oriented roughly parallel with the lakeward edge of the accreting ice mass. Each undulation marks a

short hiatus in the lakeward ice advance when freezing spray and minor amounts of wave tossed brash ice accumulate on the advancing icefront. The first ice ridge is generally the smallest of the lake ice ridges. Like its more lakeward counterparts (Fig. 3c) it has a steep nearly vertical lakeward face and a gently sloping landward surface. Both ridges are frequently reduced to grounded remnant ice blocks upon deterioration or breakup (Fig. 3d). For the discussion that follows, the ice complex at the study site is defined by the patterned combination of three features: the icefoot, the ice lagoon and the ice ridge. A schematic representation of these three structures is shown in Figure 4.

ICE CONDITIONS AND CLIMATOLOGICAL DATA

The ice conditions were categorized into five distinct stages: no ice, accretion, static, deterioration and break up. The stages of ice development used here were determined from the time lapse photography of the ice at the study site. Accretion is a visible addition of ice since the time of the previous slide while deterioration and breakup are a reduction in the ice mass. Deterioration is a gradual reduction of the ice mass apparent only after a series of slides is viewed in succession while breakup is the rapid destruction of the nearshore ice complex usually under severe lake conditions. During breakup, rapid change is visible from slide to slide and is usually exemplified by the landward displacement of the ice complex. The static condition referred to here connotates no visible change in the ice complex from slide to slide while the condition of "none" refers to the total absence of ice in the picture.

The stages of ice development were related to the following climatic conditions: wind direction, wind speed, air temperature and water temperature. Figures 5 through 10 and Appendix F show the climatic conditions as they relate to the ice conditions for January and February 1974. There does not appear to be a single climatic variable that can be correlated alone to ice development stages. The combined influence of air temperature, wind direction and wind speed control the stages of ice development in a complicated manner.

It may be considered an obvious observation that increasing or decreasing the air temperature directly influences the breakup or accretion of lake ice. During the months of January and February 1974 ice deteriorated or began to

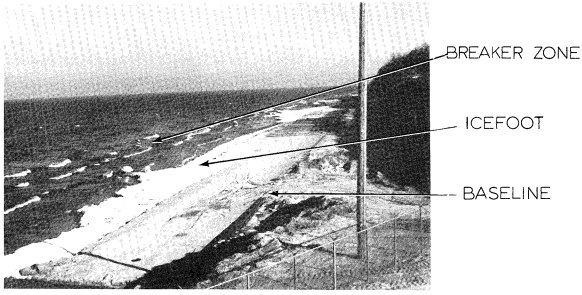

a) The baseline, icefoot and first breaker zone.

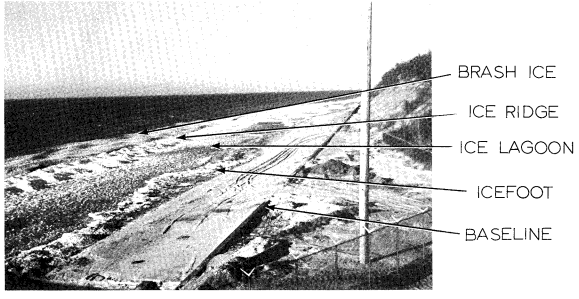

b) The baseline, icefoot, first ice lagoon, first ice ridge and floating brash ice.

FIG. 3. Characteristic ice features at various stages in the formation and breakup of the nearshore ice complex.

c) The ice complex from shore to beyond the second ice ridge.

d) Remnant ice blocks delineating the former position of the second ice ridge.

FIG. 3 continued.

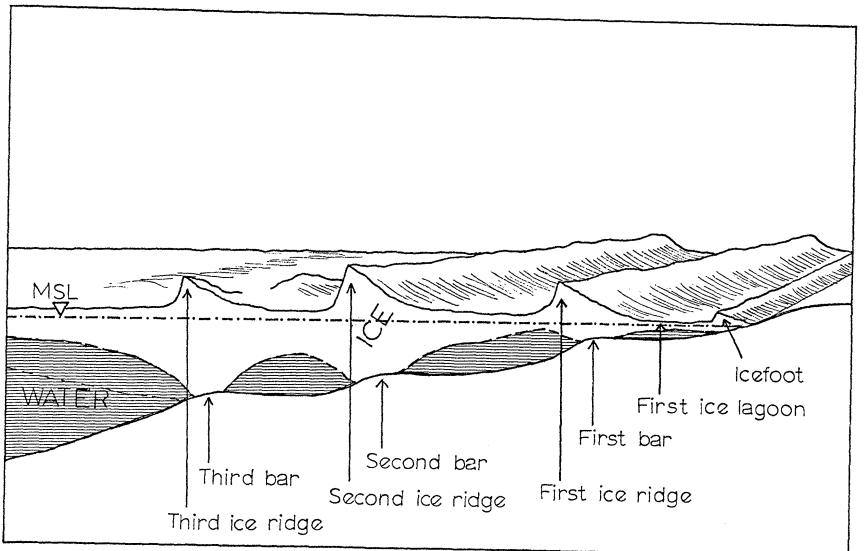

FIG. 4. Schematic representation of the typical nearshore ice complex at the study site.

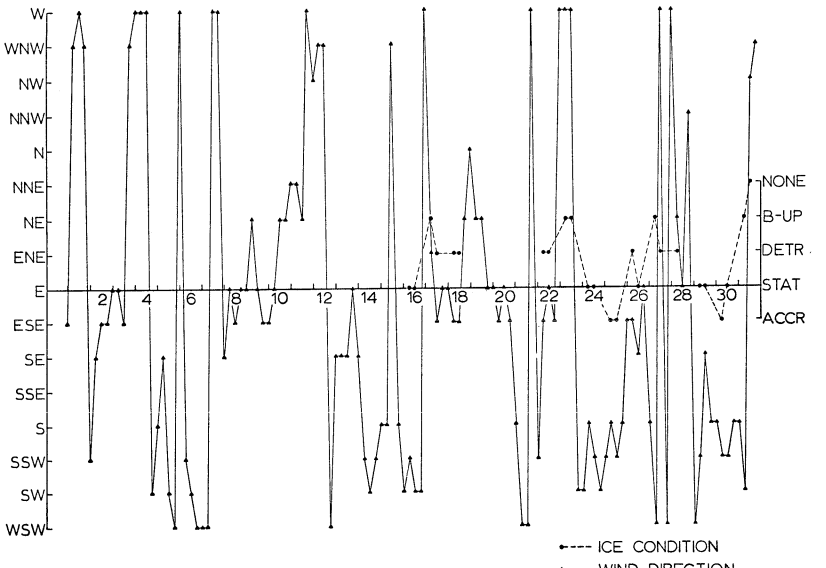

FIG. 5. Plot of ice conditions and wind direction: January 1974.

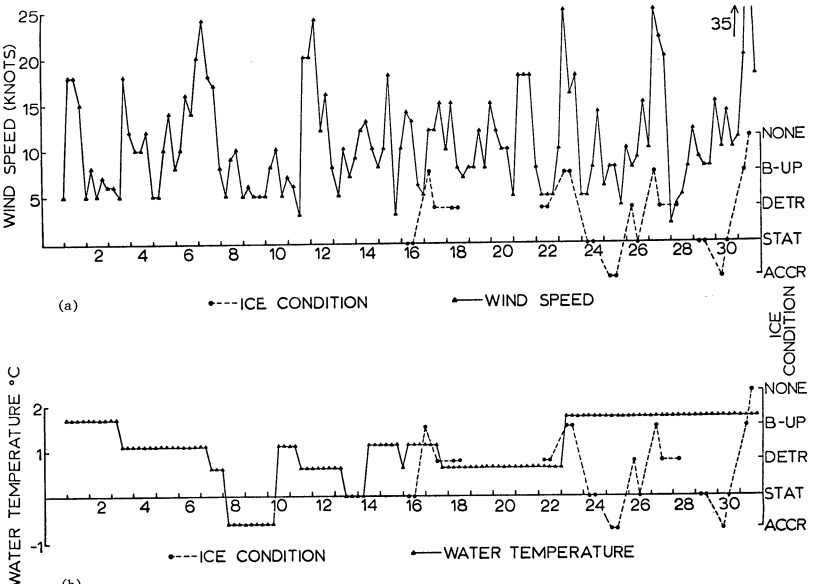

FIG. 6. Plot of ice conditions and wind speed and water temperature: January 1974.

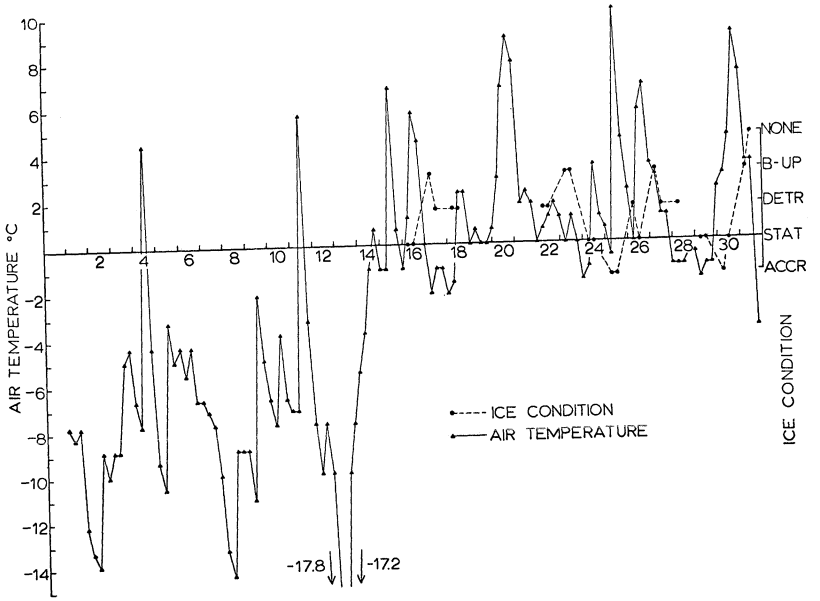

FIG. 7. Plot of ice conditions and air temperature: January 1974.

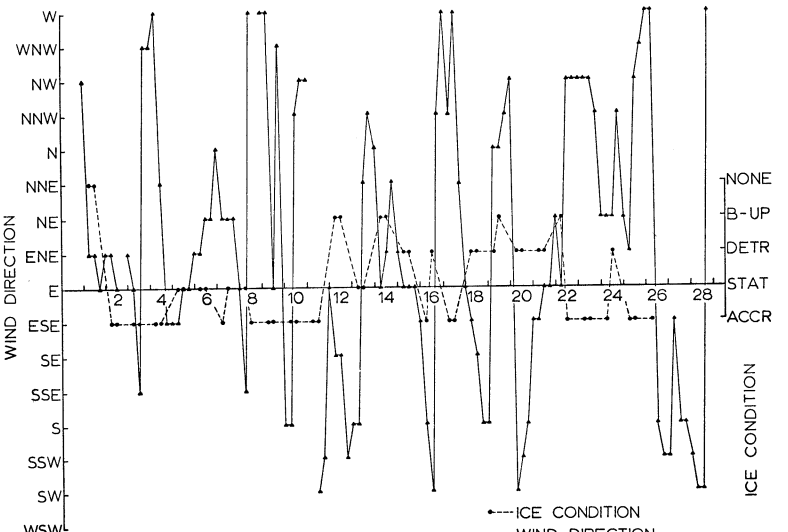

FIG. 8. Plot of ice conditions and wind direction: February 1974.

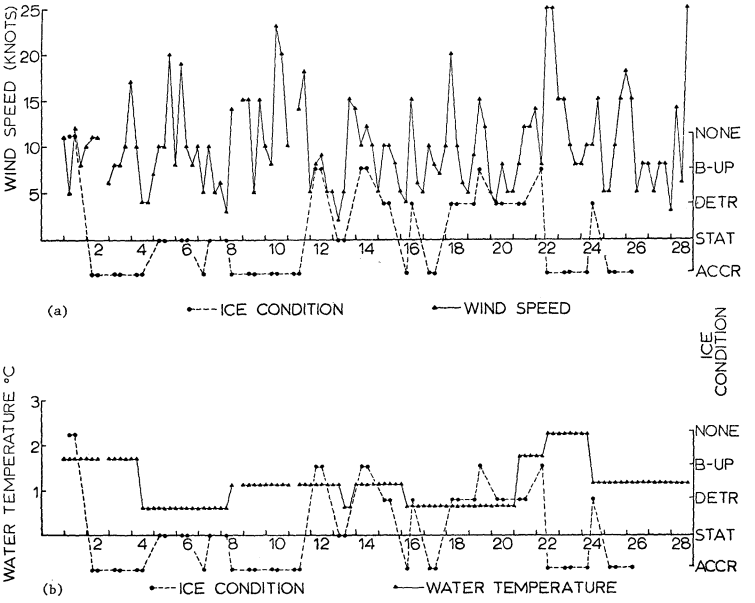

FIG. 9. Plot of ice conditions and wind speed and water temperature: February 1974.

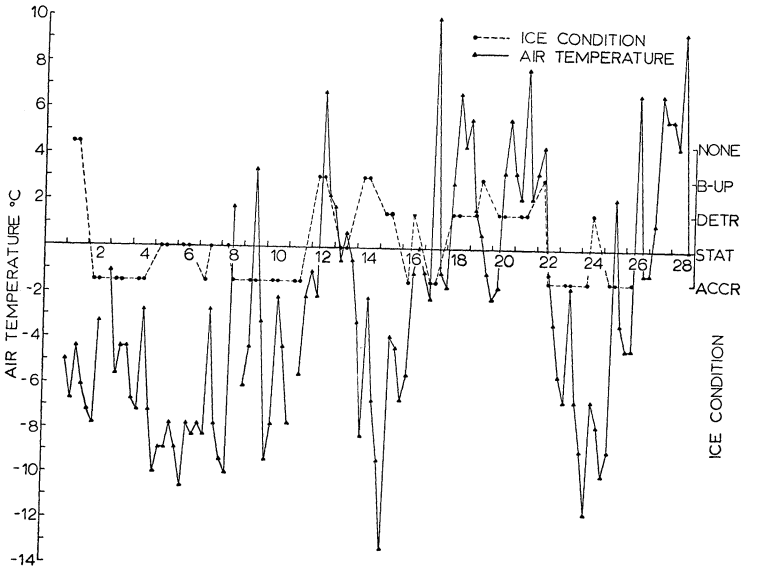

FIG. 10. Plot of ice conditions and air temperature: February 1974.

breakup shortly after an increase in air temperature. Subfreezing air temperatures usually initiated accretion; however, during the period 14-15 February 1974 ice breakup occurred despite subzero air temperatures. During this time period the water temperature remained constant but the wind direction was predominantly offshore at speeds of about 10 knots, indicating that the accretionary effect of subzero air temperatures may be negated by strong offshore winds.

The climatic variable that has the least influence on the stages of ice development defined here is the surface water temperature. Figure 6b and Figure 9b represent the surface water temperatures and the ice development stages for January and February 1974 respectively. An examination of these figures indicates a poor correlation between these variables.

To more closely examine the relationship between the climatic variables and the ice conditions we chose an accretionary sequence starting on 22 February and extending through 26 February, for which the time lapse system provided good coverage. For this period Figure 11a-d shows the ice conditions plotted against each of the climatic variables, and Figure 12 represents the ice buildup from the baseline. Several observations can be made that may lead to a better understanding of the nearshore ice development at the study site.

Immediately preceding the accretionary sequence, easterly winds and rising air temperatures produced significant overnight deterioration on 21 February 1974 and reduced the preexisting ice ridge system to grounded blocks and floating ice fragments. Rotation of wind direction to an onshore northwesterly quadrant accompanied by an increase in wind speed and a drop in air temperatures on 22 February 1974 initiated the accretive sequence. The onshore wind direction coupled with high wind speed forced the remnant ice blocks onto the beach and subsequently augmented this accumulation by moving floating brash, ball and pancake ice shoreward, producing a nearly vertical 2 meter high wall of shore ice in less than 3 hours. Rapid ice accumulation under severe lake conditions on 22 February resulted in the incorporation of large volumes of sediment in the ice giving it a gray-brown coloration. Ice formed under the less severe conditions during the remainder of the accretive sequence (23-26 February) was much whiter in color, making it easily distinguishable from the darker colored ice deposited during the storm. Although air temperatures were well below freezing, Figure 11 shows one data point (24 February) indicative

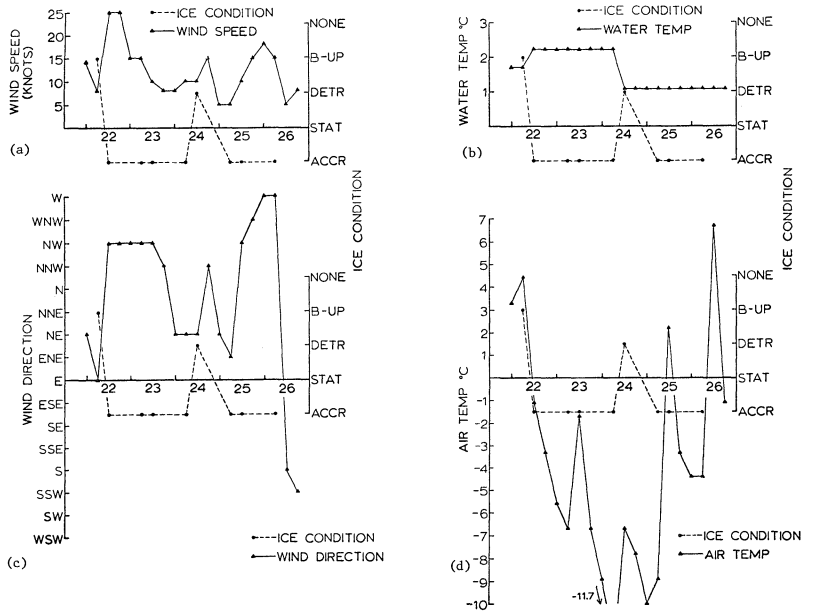

FIG. 11. Plot of climatic variables and ice conditions for the selected period of 22 February through 26 February 1974.

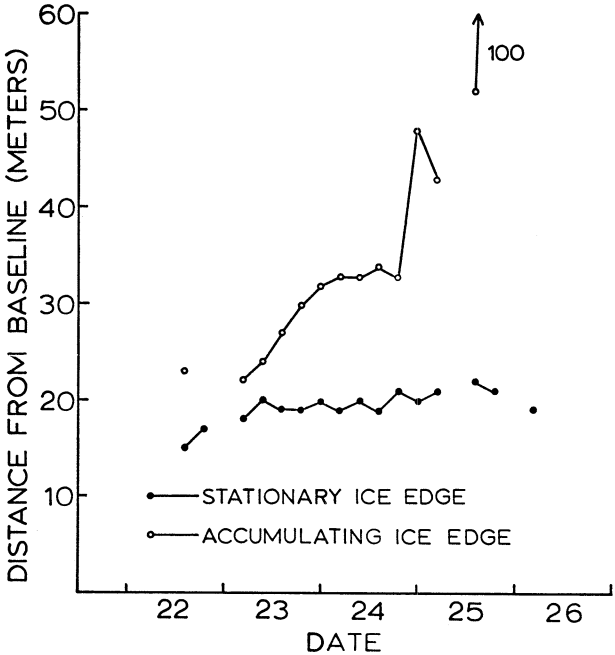

FIG. 12. Ice accretion during the period of 22 February through 26 February 1974.

of significant deterioration. This corresponds to a photograph taken just following a period of approximately 8 hours when wind direction was predominantly offshore, again demonstrating the complex interrelationship between ice stage development and climatic variables.

RIDGE LOCATION AND NEARSHORE BREAKER ZONES

One of the primary aspects of our work was oriented to the quantification of the ice ridge position during the winter season and its location relative to the nearshore breaker zones. Ayers et al. 1973 suggest that visual observation and the qualitative superimposition of slides depicting the location of the breaker zones with that of the ice ridges leads to the conclusion that the two are coincidental.

Using the oblique photographs for the winter of 1974, we measured the distance from a permanent baseline to the breaker zones and the ice ridges. The measured points are shown in Figure 13 and their values recorded in Table 1. The coincidence of the location of the breaker zones and the ice ridges is apparent. Three breaker zones and three ice ridges were identified during this winter period. The ice ridge nearest to shore and its corresponding breaker zone are best defined with the least scatter in the data points. As the distance from shore increases, coincidence between the breaker zone and ice ridges is still present but the scatter becomes much greater as summarized in Table 2.

The scatter in the data is a function of the analysis and the real variability in the mean position of the ice ridge, breaker zone and nearshore bars. Each variable is positioned within a linear zone and its location is approximated by a line for measurement purposes. In particular, the breaker zone (offshore bar) has a natural width and since its location is defined by only one slide at a given time, this location is dependent upon wave conditions as well as the position of the breaking wave at the time of photo exposure. It follows that one photo at any given time is not sufficient to define the range in width of this zone. The position of an ice ridge is more definitive since grounded remnant ice blocks (Fig. 3d) maintain their position during breakup. Frequently wave activity breaches an ice ridge providing a cross-sectional view and revealing its mid-ridge intersection with the water surface.

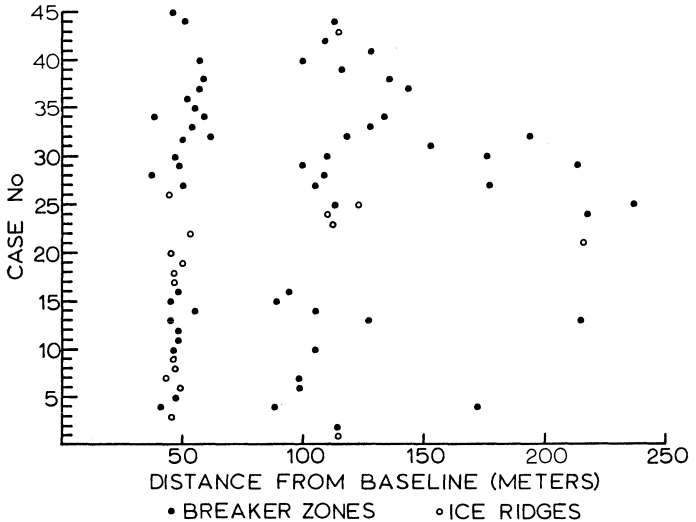

FIG. 13. Plot of the location of breaker zones and ice ridges for the analyzed photographs.

TABLE 1. Identification of the case numbers used in Figure 13.

Case	Slide No.	Date	0-75 Meters		76-150 Meters		151-300 Meters	
			Breaker Zone	Ice Ridge	Breaker Zone	Ice Ridge	Breaker Zone	Ice Ridge
1	CM-9-74-23	1-17-24				114		
2	CM-10-74-2	1-22-74			114			
3	CM-10-74-3	1-22-74		45				
4	CM-10-74-9	1-23-74	41		88		172	
5	CM-10-74-18	1-24-74	47					
6	CM-10-74-20	1-25-74		49	98			
7	CM-10-74-22	1-25-74		43	98			
8	CM-10-74-23	1-25-74		47				
9	CM-10-74-28	1-26-74		46				
10	CM-10-74-29	1-27-74	46		105			
11	CM-11-74-5	1-29-74	48					
12	CM-11-74-6	1-30-74	48					
13	CM-11-74-13	1-31-74	45		127		215	
14	CM-11-74-30	2-3-74	55		105			
15	CM-11-74-32	2-4-74	45		89			
16	CM-12-74-12	2-7-74	48		94			
17	CM-12-74-18	2-8-74		46				
18	CM-12-74-20	2-8-74		46				
19	CM-12-74-29	2-10-74		50				
20	CM-13-74-13	2-14-74		45				
21	CM-13-74-19	2-15-74						216
22	CM-13-74-24	2-16-74		53				
23	CM-13-74-26	2-17-74				112		
24	CM-14-74-2	2-19-74				110	218	
25	CM-14-74-3	2-19-74			113	123	237	
26	CM-14-74-15	2-22-74		44				
27	CM-14-74-16	2-22-74	50		105		177	
28	CM-14-74-17	2-22-74	37		109			
29	CM-14-74-18	2-22-74	49		100		214	
30	CM-14-74-19	2-22-74	47		110		176	
31	CM-14-74-21	2-23-74	55				153, 270	
32	CM-14-74-22	2-23-74	62		118		194	
33	CM-14-74-23	2-23-74	54		128			
34	CM-14-74-24	2-23-74	38, 59		134			
35	CM-14-74-26	2-24-74	55					
36	CM-14-74-27	2-24-74	52					
37	CM-14-74-28	2-24-74	57		144			
38	CM-14-74-29	2-24-74	59		136			
39	CM-14-74-30	2-25-74			116			
40	CM-14-74-31	2-25-74	57		100			
41	CM-14-74-33	2-25-74			123			
42	CM-14-74-34	2-25-74			109			
43	CM-14-74-36	2-26-74				115		
44	CM-17-74-3	3-13-74	51		113			
45	CM-18-74-5	3-20-74	46					

TABLE 2. Statistical summary of breaker zone and ice ridge locations.

	DISTANCE FROM BASELINE (METERS)								
	0-75			76-150			151-300		
	n	$\bar{x}$	S_x	n	$\bar{x}$	S_x	n	$\bar{x}$	S_x
BREAKER ZONES	25	50	7	24	112	15	10	203	35
ICE RIDGES	11	47	3	5	115	5	1	216	

n = number of cases

$$\bar{x} = \left(\sum_{i=1}^{n} x_i \right) \Big/ n$$

$$S_x^2 = \frac{\sum_{i=1}^{n} (x_i^2) - \left(\sum_{i=1}^{n} x_i \right)^2 \Big/ n}{n - 1}$$

This breached cross-section maintains its position in several slides allowing calculation of both the ice ridge's position and height.

The position of the breaker zones is known to reflect the position of the offshore bar system. The clear relationship between the offshore ice ridges and the breaker zones leads to the conclusion that ice ridges are coincidental with the bar systems. The time lapse photographs of the nearshore ice complex indicate that once established the ice ridges remain stationary for longer

periods than the intervening lagoons. This suggests that not only are the ice ridges greater in thickness than the ice lagoons but that they are situated directly on the nearshore lake bottom. On one occasion, O'Hara and Ayers (1972) verified during diving operations that the remnant blocks of a deteriorating ice ridge were embedded in the bottom. Bryan and Marcus (1972) observed remnant ice blocks grounded along offshore bars during an aerial reconnaissance.

NEARSHORE EROSION

Seibel (1972) formulated that the ice ridge formation and ice ridge breakup are an integral part of the modification of offshore topography and aggravation of shoreline erosion. Scour of the nearshore topography is inevitable at the position of the ice ridges. The influence of the modification on the shoreline and bluffline is unknown. It is speculated that a storm immediately following breakup could cause greater damage along the shoreline than a storm of equal magnitude several weeks after breakup when the nearshore bars have had a sufficient opportunity to reform.

It has been clearly observed by ourselves and others that large quantities of sediment are incorporated in the nearshore ice complex during accretionary stages. At the time of breakup this ice-locked sediment was transported landward, lakeward or alongshore. The combined effect of ice rafting and scour suggest that nearshore ice plays a greater than anticipated role in modifying the nearshore topography.

CONCLUSION

Several pertinent conclusions appear to be evident from the monitoring of the nearshore ice on this portion of southeastern Lake Michigan:

1. The computer analysis of the time lapse high oblique photographs provided the basis for a quantitative analysis of the hypothesis of coincident location of offshore ice ridges, offshore bars, and breaker zones.

2. The data reveal that the three above characteristic shore features are indeed coincident.

3. The stages of ice development are not controlled by any single

climatic variable but instead there exists a complex interrelationship between the two.

4. Easterly winds coupled with rising air temperatures appear to consistently produce significant deterioration of the ice complex.

5. Onshore northwesterly winds coupled with increase in wind speed and a drop in air temperature initiate accretive sequences.

6. Large quantities of sediment are incorporated in the nearshore ice complex during accretionary stages and are transported landward, lakeward or alongshore at the time of breakup.

7. Since the ice ridges are grounded, as the data indicate, they may serve to modify the nearshore topography in the proximity of the offshore bars sufficiently to influence the wave regime capable of reaching and acting on the shoreline and bluffline. The exact influence of this modification of the shoreline and bluffline is not yet established.

REFERENCES

American Society of Photogrammetry. 1966. Manual of Photogrammetry, 3rd ed., 2 vols. Washington, D. C. 1199 p.

Ayers, J. C., N. W. O'Hara and W. L. Yocum. 1971. Benton Harbor Power Plant Limnological Studies, Part VIII: Winter operations 1970-71. Univ. Michigan, Great Lakes Res. Div. Spec. Rep. No. 44. 37 p.

Ayers, J. C. and W. L. Yocum. 1972. Benton Harbor Power Plant Limnological Studies, Part XI: Winter operations 1971-72. Univ. Michigan, Great Lakes Res. Div. Spec. Rep. 44. 22 p.

Ayers, J. C., W. L. Yocum and E. Seibel. 1973. Benton Harbor Power Plant Limnological Studies, Part XIV: Winter operations 1972-73. Univ. Michigan, Great Lakes Res. Div. Spec. Rep. No. 44. 22 p.

Bryan, L. M. and M. G. Marcus. 1972. Physical characteristics of near-shore ice ridges. Arctic 25: (3)182-192.

Evenson, E. B. 1973. The ice-foot complex: Its morphology, classification, mode of formation, and importance as a sediment transporting agent. Papers of the Michigan Acad. Sci., Arts and Letters, vol. VI, no. L. p. 43-57.

Heap, J. A. 1963. Some characteristics of the winter ice cover of Lake Michigan, 1962-63. Univ. Michigan, Great Lakes Res. Div. Pub. No. 10. p. 216-218.

Heap, J. A. and V. E. Noble. 1966. Growth of ice on Lake Michigan. Univ. Michigan, Great Lakes Res. Div. Spec. Rep. No. 26. 94 p.

Kivisild, H. R. 1970. River and lake ice terminology, *in* Ice and its action on hydraulic structures. IAHR Symposium, Reykjavik, Iceland, 7-10 September 1970. p. 1-12.

Maresca, J. W., Jr. 1975. Bluffline recession, beach change, and nearshore change related to storm passages along southeastern Lake Michigan. Ph.D. Dissertation, Univ. Michigan, Ann Arbor. 481 p.

Marsh, W. M., B. D. Marsh and J. Dozier. 1973. Formation, structure, and geomorphic influence of Lake Superior icefoots. Amer. J. Sci. 273: 48-64.

Marshall, E. W. 1966. Air photo interpretation of Great Lakes ice features. Univ. Michigan, Great Lakes Res. Div. Spec. Rep. No. 25. 92 p.

O'Hara, N. W. and J. C. Ayers. 1972. Stages of shore ice development. Proc. 15th Conf. Great Lakes Res., Internat. Assoc. Great Lakes Res. p. 521-535.

Olson, C. 1973. Class notes from Natural Resources 442, Univ. Michigan, Ann Arbor.

Seibel, E. 1972. Shore erosion at selected sites along Lakes Michigan and Huron. Ph.D. Dissertation, Univ. Michigan. 175 p.

APPENDIX A. DAILY ICE CONDITIONS

17 January 1974 (CM-9-74-23)	The first photo taken from the camera monitor system and utilized in this study was exposed 17 January 1974. Evident in the photo was the deteriorated first ice ridge, discolored due to sedimentary lag deposits. The second lagoon had been reduced to floating brash ice and the position of the second ridge was marked by grounded remnant ice blocks of average height 1.4 m. The remnant ice fragments of the second lagoon are absent in photos taken later on 17 January 1974.
18 January 1974	There was continued deterioration of the first ridge and the remnant blocks of the second ice ridge.
19-21 January 1974	No photos were available for these three days.
22 January 1974 (CM-10-74-2,3)	Waves displaced the ice blocks formerly marking the position of the second ridge and rapidly reduced the first ridge to a narrow band of intermittently breached, grounded ice.
23 January 1974 (CM-10-74-9)	Overnight wave activity further reduced the first ridge to ice fragments and ice blocks of average height 1.3 m grounded along the shoreline. Wave action and continued influx of brash ice rebuilt the ice foot at the water's edge.
24 January 1974 (CM-10-74-18)	Little change in the ice complex since 23 January. The lakeward edge of the icefoot had become more irregular in plan and the few isolated blocks of ice formerly located between the plunge zone and the icefoot were no longer present.
25 January 1974 (CM-10-74-20,22, 23)	Overnight ice accretion resulted in the formation of the first lagoon and the first ice ridge. The lagoon is composed of unconsolidated brash ice isolated behind the wave resistant first ridge. A band of slush ice was present lakeward of the first ice ridge. The first ridge was augmented by freezing spray and wave tossed slush ice which caused it to narrow and increase in height.
26 January 1974 (CM-10-74-28)	The band of slush ice lakeward of the first ice ridge dissipated overnight and the deterioration of the lakeward edge of the first ridge accented its irregularity in plan. The icefoot visibly deteriorated.
27 January 1974 (CM-10-74-29)	Overnight wave action broke up the first ridge and piled the ice fragments on the shore rejuvenating the icefoot. The intermittent patches of slush ice present in photos taken early 27 January 1974 were absent in later photos taken that day and the icefoot showed visible wave induced deterioration as the day progressed.

28 January 1974	The ice conditions remained visibly unchanged other than a light snow cover.
29 January 1974 (CM-11-74-5)	Wave action eroded the lakeward edge of the icefoot back to a position behind the waterline. This deterioration continued until both the waterline and a narrow, irregular strip of beach were visible behind the icefoot in the last photo taken 29 January 1974.
30 January 1974 (CM-11-74-6)	Approximately 21 m of overnight fast ice accretion advanced the lakeward edge of the fast ice to a location just shoreward of the first breaker zone, no ice ridge was present. There was little further change in the ice conditions on 30 January 1974.
31 January 1974 (CM-11-74-13)	Northwesterly winds broke-up the fast ice overnight rebuilding the icefoot, the only ice feature visible in the first photo taken 31 January. The intense wave activity during the balance of the day finally reduced the icefoot to fragments which were washed onto the beach.
1 February 1974	The only remaining ice consisted of the remnant fragments of the icefoot covered by a light overnight snow.
2 February 1974	Light wave conditions and the constant influx of small quantities slush ice resulted in the slow formation of a small icefoot approximately 0.5 m high as the day progressed.
3 February 1974 (CM-11-74-30)	The first two photos taken 3 February documented the continued growth of the icefoot and the formation of small ice lobes on its lakeward edge. The increase in wave activity later in the day deteriorated the icefoot and produced a very irregular shape in plan. The icefoot was discolored due to the incorporation of sediment in the ice.
4 February 1974 (CM-11-74-32)	Approximately 18 m of overnight fast ice accretion but no ridges were identifiable in early photos taken on this date. The height of the lakeward edge of the fast ice was increased by wave tossed brash ice, freezing spray generated by waves striking the ice formation and from recently developed blowholes.
5 February 1974	No visible change in the ice conditions during this day.
6 February 1974	Although wave intensity was low, wave splash and wave tossed slush ice slowly increased the height of the lakeward edge of the fast ice. New ice along the edge was darker than the rest of the snow covered fast ice indicating sediment incorporation into the ice.
7 February 1974 (CM-12-74-12)	Approximately 8 m of fast ice accretion overnight. The newly accreted ice was much whiter in color than the former lakeward edge of the fast ice making the boundary easily

	distinguishable. Numerous blowhole cones were visible in photos taken on this date.
8 February 1974 (CM-12-74-18,20)	Slush ice was visible near the horizon in the first photo taken 8 February and brash ice had begun to accumulate in a narrow band approximately 19 m wide just lakeward of the fast ice, but separated from it by a zone of open water. The last photo taken 8 February showed that slush ice covered the entire lake and the band of accumulating brash ice had widened and consolidated. The narrow band of semi-consolidated brash ice remained isolated from the fast ice by the intermediate zone of the slush ice - water mixture.
9 February 1974	The entire lake was ice covered in the first photo taken this day. By midday drifting pancake ice was produced by the breakup evident in a zone lakeward of the main body of fast ice. The last photo taken 9 February showed the zone of floating brash ice had begun to reconsolidate.
10 February 1974 (CM-12-74-29)	The lake was ice covered to the horizon in photos exposed early in the day, later photos show the horizon was icefree. A small ice ridge had begun to form over the former position of the first breaker zone, the location previously occupied by the band of brash ice evident in the photos taken 8 February.
11 February 1974	Open water was visible near the horizon in the first photo taken on 11 February although later photos showed the lake was ice covered to the horizon. There was overnight enlargement of the new ridge which had become evident in slides taken 10 February.
12 February 1974	A zone of open water formed near the horizon, its size did not appear to vary appreciably during the day. Otherwise there was no visible change in the other ice structures. Sun rot had continued to concentrate lag deposits around blow holes in the fast ice.
13 February 1974	The area of ice-free water evident near the horizon in photos taken 12 February was barely visible due to both its reduction in size and the foggy conditions which existed during the time of the midday photo exposure. A narrow strip of open water separated the fast ice from the shore at the waterline. This may have been an atypical feature resulting from minor quantities of effluent discharge below the field of view at the bottom of the photos.
14 February 1974 (CM-13-74-13)	The ice broke up into pancake and floating brash ice, resulting in a wide zone of open water bounded by floe ice near the horizon and the fast ice at the shore. Ice blocks were grounded along a line marking the position occupied by a breaker zone in previous slides.

15 February 1974 (CM-13-74-19)	The fast ice and grounded ice blocks were still present in photos taken this day. The lake was otherwise ice-free to the horizon since the floe ice located near the horizon in photos taken 14 February had been dispersed overnight by easterly winds.
16 February 1974 (CM-13-74-24)	The first photo taken this day showed brash ice had begun to accumulate in a band adjacent to the lakeward edge of the fast ice. Waves forced the brash ice shoreward forming a small ridge located over the position of the first breaker zone. The newly forming ridge initially remained isolated from the fast ice by a zone of relatively ice free water but was later forced nearer to the fast ice by increased wave action. The grounded blocks of ice became more scattered by the end of the day and appeared to have moved in a northerly longshore direction.
17 February 1974 (CM-13-74-26)	Overnight ice accretion of approximately 217 m resulted in the formation of the second and third lagoons and the second ice ridge. Numerous blow holes had formed along the second ridge by the time the last photo was taken on 17 February.
18 February 1974	The third lagoon was broken up and dispersed overnight and a breach had developed in the second ice ridge. During the course of the day the second lagoon deteriorated into floating brash ice trapped between the fast ice and the second ice ridge. There was visible concentration of lag deposits along the fast ice located shoreward of the first ice ridge, particularly around the blow hole cones.
19 February 1974 (CM-14-74-2,3)	Wave activity during the course of the day broke up the second ice ridge and second lagoon. The resulting ice blocks and fragments were piled on the lakeward edge of the first ice ridge. During breakup a breach in the second ridge allowed observation of a wave breaking at a location similar to that of the second ridge.
20 February 1974	Little major change occurred in the ice conditions on 20 February. There was visible fluctuation of a zone of brash ice adjacent to the lakeward edge of the fast ice. Blow hole cones darkened as the minor snow cover melted from the ice surface and sun rot further concentrated lag deposits.
21 February 1974	High air temperatures and easterly winds severely deteriorated the remaining nearshore ice. Sandy lag deposits darkened the ice surface and a zone of open water developed between the remaining ice and the shoreline.
22 February 1974 (CM-14-74-15,16, 17,18,19)	Wave activity and a rise in air temperature the previous night reduced the remaining ice to grounded blocks approximately 1.1 m high and floating brash ice confined between the blocks and the shoreline. Storm conditions which

developed later in the morning forced the remaining ice onto the beach and formed lobes of ice along the shore as high as 1.7 m. Subsequently the influx of storm driven ice filled these irregularities in the lakeward edge of the accreting ice front. The last photo taken on 22 February showed a massive, gray white accumulation of shore ice, having a relatively smooth lakeward edge in plan that was still being augmented by wave tossed ice fragments.

23 February 1974 (CM-14-74-21,22, 23,24)

The wave activity diminished during the night and the first slide taken on 23 February showed some minor accretion to the fast ice. Due to the incorporation of sediment, the ice deposited during the storm had a greyish-brown coloration in contrast to the lighter colored ice accreted later under calmer lake conditions. Photos taken early 23 February show patches of brash ice adjacent to the lakeward edge of the fast ice. Slow accretion throughout the day was evident as the white lamination of new ice widened along the lakeward edge of the fast ice.

24 February 1974 (CM-14-74-26,27, 28,29)

The first slide taken 24 February showed significant overnight ice accretion and a narrow zone of floating slush ice just lakeward of the fast ice. Wave tossed ice fragments and freezing spray augmented the fast ice, and subsequent minor wave activity produced blowholes and an irregular shape in plan along the lakeward edge of the fast ice. By the time the last photo was exposed 24 February the blowhole cones, located near the edge of the fast ice, were numerous and well developed.

25 February 1974 (CM-14-74-30,31, 33,34)

The first slide taken 25 February showed approximately 15 m of overnight ice accretion and slush ice near the horizon. The slush ice covered the lake to the horizon by early afternoon, and increased in concentration by late afternoon. The last slide taken on 25 February showed the lake covered with brash ice to the apparent horizon. A very dense zone of brash ice was bounded by the fast ice and the second breaker zone which was marked by a gentle roll on the slushy water surface.

26 February 1974 (CM-14-74-36)

Due to camera malfunction only two morning slides were available for the evaluation of the ice conditions on 26 February. The lake was covered with ice to the horizon and various stages of lake ice development were visible. The extinct blow holes were evident lakeward of the greyish storm deposited fast ice. Undulations created by freezing spray and wave tossed brash ice visible along the ice surface marked stationary periods in the lakeward advance of the fast ice. A small ridge was forming over the position formerly occupied by the second breaker zone.

(CM-15-74)	Due to camera malfunction the CM-15-74 slide series depicting the breakup sequence of the lake ice was lost. The first slide taken after camera repair was CM-16-74-1. Slides were selected at one week intervals, representing the same time of day, until the study area was totally ice-free.
6 March 1974 (CM-16-74-1)	The lake was totally devoid of ice to the horizon. The remaining shore ice abruptly truncated at the waterline forming a nearly vertical lakeward face. The shoreward edge of the ice was irregular in plan and covered portions of the baseline (seawall). The entire ice body was dark brown in color due to large quantities of sediment concentrated on the ice surface by sun rot of the ice. A large continuous crack extending parallel with the lakeward edge of the deteriorating ice was indicative of undercutting by waves and resulted in the subsequent collapse of the undercut portion.
13 March 1974 (CM-17-74-3)	Significant narrowing of the shore ice had taken place since 6 March 1974. The lakeward edge of the shore ice had retreated shoreward exposing the waterline and the concentration of sandy lag deposits had further darkened the surface of the ice body.
20 March 1974 (CM-18-74-5)	Both edges of the remnant shore ice were very irregular in plan. The lakeward edge of the sediment darkened ice was located well behind the waterline.
27 March 1974 (CM-19-74-5)	Further visible reduction in the overall mass of the deteriorating ice body was apparent in photos taken on 27 March. The remnant ice now appeared as a series of connected ice mounds ranging in height from 0.4 m to 1.1 m.
3 April 1974 (CM-20-74-4)	By 3 April the shore ice had deteriorated into randomly scattered mounds of ice of variable size and shape nearly black in color indicating the presence of heavy minerals in the lag deposits.
6 April 1974 (CM-20-74-16)	The study area was totally devoid of any ice.

APPENDIX B. DESCRIPTION OF SLIDES USED IN ANALYSIS

Terminology Used in Slide Description

SLIDE NUMBER: The slide description is presented in order by slide number. Each camera monitor slide is coded by roll number, year and exposure number.

TIME:
- E-AM: early morning
- L-AM: late morning
- NOON: midday
- E-PM: early afternoon
- L-PM: late afternoon

ACCRETION: A visible lakeward advance of the ice front.

DETERIORATION: A gradual decay of the nearshore ice complex apparent only after viewing several slides in sequence.

BREAKUP: A rapid decay and dispersal of the nearshore ice usually taking place in the period of a few hours.

ICEFOOT: A small ridge-like ice structure which forms at the waterline.

ICE LAGOON: A tabular ice formation which shows little vertical relief and is confined between the icefoot and first ice ridge or between two ice ridges.

ICE RIDGE: A linear ice structure having variable vertical relief and usually aligned parallel with the shoreline. A cross-sectional view would show a nearly vertical lakeward face and more gently sloping landward face.

FAST ICE: An ice formation which has greater thickness than an ice lagoon and which extends from the icefoot nearly to the location of the first offshore bar.

SHORE ICE: An ice mass which has been deposited on the beach and is terminated near the waterline.

BRASH ICE: Floating, unconsolidated ice fragments usually formed offshore or produced by the break-up of an ice system.

SLUSH ICE: A floating, unconsolidated ice-water mixture often produced on the lake surface during snowfalls.

1. CM-9-23-74 (17 January 1974, E-PM) — Extinct blowholes were observed along the first ice ridge, which was discolored due to the concentration of sandy lag deposits by sun rot of the ice. Grounded, isolated ice blocks marked the former position of the second ice ridge. The second ice lagoon had been reduced to floating ice fragments.

2.	CM-10-74-2 (22 January 1974, E-AM)	The lakeward edge of the first ice ridge was deteriorated sufficiently to expose the first breaker zone. The second breaker zone was also defined in the photo.
3.	CM-10-74-3 (22 January 1974, L-AM)	Waves breached the first ice ridge showing its mid-ridge location relative to the baseline where intersection of the ridge with the water surface was evident.
4.	CM-10-74-9 (23 January 1974, L-AM)	The first, second and third breaker zones were observable lakeward of the ice blocks which were remnants of the first ice ridge. Ice fragments derived from the break of the first ridge rejuvinated the icefoot.
5.	CM-10-74-18 (24 January 1974, L-PM)	The first breaker zone was visible lakeward of the icefoot located at the waterline.
6.	CM-10-74-20 (25 January 1974, E-AM)	Overnight ice formation produced the first ice lagoon, composed of floating brash ice, and the first ice ridge. A zone of floating slush ice was present lakeward of the first ice ridge.
7.	CM-10-74-22 (25 January 1974, E-PM)	The first ice ridge narrowed and its shoreward face steepened. The first ice lagoon appeared less consolidated than in the previous slide.
8.	CM-10-74-23 (25 January 1974, L-PM)	The icefoot and first ice lagoon deteriorated while wave tossed ice fragments augmented the first ice ridge increasing its width.
9.	CM-10-74-28 (26 January 1974, L-PM)	The icefoot and first ice ridge showed extensive deterioration and the first lagoon deteriorated into slush ice.
10.	CM-10-74-29 (27 January 1974, E-AM)	Overnight wave activity brokeup the first ice ridge and rejuvinated the icefoot. The plunge zone, first and second breaker zones were observable.
11.	CM-11-74-5 (29 January 1974, L-PM)	The first breaker zone and waterline were visible lakeward of the deteriorated icefoot.
12.	CM-11-74-6 (30 January 1974, E-AM)	Due to overnight ice accretion, the lakeward edge of the fast ice was located near the first breaker zone.
13.	CM-11-74-13 (31 January 1974, NOON)	Wave activity overnight reduced the fast ice to fragments deposited on the beach. The plunge zone and three breaker zones were defined.
14.	CM-11-74-30 (3 February 1974, L-PM)	The plunge zone and first and second breaker zones were visible lakeward of the deteriorated icefoot.

15. CM-11-74-32 (4 February 1974, L-AM) — The first breaker zone was defined just lakeward of the fast ice which formed overnight.

16. CM-12-74-12 (7 February 1974, L-AM) — New fast ice formed nearly to the position of the first breaker zone and blowholes were present along the fast ice surface. The first and second breaker zones were visible in the slide.

17. CM-12-74-18 (8 February 1974, NOON) — Slush ice was observed covering the lake surface near the apparent horizon. A zone of slush ice had begun to consolidate just lakeward of the static fast ice.

18. CM-12-74-20 (8 February 1974, L-PM) — The accumulation of ice on the lake surface near the apparent horizon had consolidated. Brash ice concentrated in a band approximately 42 m wide, parallel to the lakeward edge of the fast ice.

19. CM-12-74-29 (10 February 1974, E-PM) — Extinct blowholes were noted along the surface of the stationary fast ice. The lake was ice covered nearly to the apparent horizon and a small ice ridge had formed just lakeward of the fast ice.

20. CM-13-74-13 (14 February 1974, NOON) — Breakup produced a large zone of open water bounded on one side by the fast ice and on the other by floating ice on the lake surface near the apparent horizon.

21. CM-13-74-19 (15 February 1974, E-PM) — The icefoot and fast ice showed further deterioration, and sun rot had concentrated sandy lag deposits around the extinct blowhole cones. A line of grounded ice blocks were observed approximately 216 m from the baseline.

22. CM-13-74-24 (16 February 1974, E-PM) — A small ice ridge was forming just lakeward of the grounded fast ice. Numerous randomly scattered ice blocks were visible well off shore.

23. CM-13-74-26 (17 February 1974, E-PM) — Overnight ice accretion formed the second ice ridge and second ice lagoon.

24. CM-14-74-2 (19 February 1974, NOON) — The third ice lagoon broke up and the second ice ridge was breached by waves. The third breaker zone was visible.

25. CM-14-74-3 (19 February 1974, E-PM) — Ice fragments derived from the breakup of the third ice lagoon and breached portions of the second ice ridge were forced shoreward by waves. A wave was observed breaking through a breach in the second ice ridge.

26. CM-14-74-15 (22 February 1974, E-AM) — Grounded remnant ice blocks marked the position of the first ice ridge.

27.	CM-14-74-16 (22 February 1974, L-AM)	Storm conditions developed forcing all ice fragments and ice blocks onto the beach. The first, second and third breaker zones were observed in the slide.
28.	CM-14-74-17 (22 February 1974, NOON)	Large volumes of floating brash ice were forced shoreward by NNW winds forming lobes of ice on the shoreline nearly 2 m high. The entire beach was ice covered and the lakeward edge of the shore ice was very irregular in plan.
29.	CM-14-74-18 (22 February 1974, E-PM)	Persisting storm conditions continued to augment the shore ice with freezing spray and wave tossed pancake, ball and brash ice. The continual influx of ice fragments filled the cusps in the lakeward edge of the shore ice.
30.	CM-14-74-19 (22 February 1974, L-PM)	Although storm conditions were beginning to subside, three breaker zones were still evident and large quantities of floating brash ice continued to augment the fast ice complex.
31.	CM-14-74-21 (23 February 1974, L-AM)	Three breaker zones were defined as well as slush ice on the lake surface near the apparent horizon. The large volumes of sediment incorporated in the fast ice deposited under storm conditions gave it a grey coloration. The lamination of ice which formed along the lakeward edge of the fast ice overnight was much whiter making it easily distinguishable from the ice deposited during the storm.
32.	CM-14-74-22 (23 February 1974, NOON)	Further accretion of ice was evident along the lakeward edge of the fast ice. Two breaker zones were evident.
33.	CM-14-74-23 (23 February 1974, E-PM)	The plunge zone and first two breaker zones were observed as well as additional ice accretion.
34.	CM-14-74-24 (23 February 1974, L-PM)	The plunge zone and first two breaker zones appeared in the slide.
35.	CM-14-74-26 (24 February 1974, L-AM)	The first breaker zone was evident as well as minor wave deterioration of the lakeward edge of the fast ice.
36.	CM-14-74-27 (24 February 1974, NOON)	Further wave deterioration of the ice edge was noted. Floating ice fragments were confined between the fast ice and the first breaker zone.
37.	CM-14-74-28 (24 February 1974, E-PM)	Continued deterioration of the lakeward edge of the fast ice resulted in an irregular contour in plan. Further blowhole development indicated the waves had undercut the lakeward boundary of the fast ice.

38. CM-14-74-29 (24 February 1974, L-PM) — First and second breaker zones were defined lakeward of the fast ice. Brash ice was accumulating between the fast ice and the first breaker zone. Blowhole cones were aligned along the outer edge of the fast ice.

39. CM-14-74-30 (25 February 1974, E-AM) — Overnight ice accretion moved the lakeward edge of the fast ice well behind the line of blowhole cones which previously marked the furthest lakeward extent of the ice.

40. CM-14-74-31 (25 February 1974, L-AM) — Little observable change in the variables since the last slide. The first and second breaker zones were defined and patches of floating ice fragments were seen on the lake surface.

41. CM-14-74-33 (25 February 1974, E-PM) — The lake was covered with unconsolidated slush ice to the apparent horizon. The second breaker zone was still observable.

42. CM-14-74-34 (25 February 1974, L-PM) — The lake surface was covered with a dense cover of brash ice to the apparent horizon. The second breaker zone was defined by a non-breaking roll on the slush ice covered lake surface.

43. CM-14-74-36 (26 February 1974, L-AM) — The lake was ice covered to the apparent horizon. A small ice ridge had begun to form over the position of the second breaker zone.

NOTE: The series of slides (CM-15-74) depicting the deterioration and break-up of the previous lake ice was lost due to camera malfunction. The following slides represented one week intervals beginning with the first slide available following repair of the time-lapse photo system. The slides were selected to represent as nearly as possible the same time of day.

44. CM-16-74-1 (6 March 1974, E-PM) — The lake was ice-free to the apparent horizon, the only remaining ice was grounded on the beach. The sediment incorporated in the ice at the time of deposition had been concentrated on the ice surface by sun rot. The large quantity of sediment deposited with the ice under storm conditions was evident in the slide.

45. CM-17-74-3 (13 March 1974, E-PM) — Remnant shore ice was confined between the seawall (baseline) and the waterline. The edge of the shore ice near the waterline had been undercut by waves.

46. CM-18-74-5 (20 March 1974, E-PM) — The remnant shore ice was extremely dark in color due to sedimentary lag deposit concentration. Wave activity eroded the lakeward edge of the shore ice to a position well behind the waterline.

47. CM-19-74-5 (27 March 1974, E-PM) — Further deterioration of the remnant shore ice with increased concentration of lag deposits was evident.

48. CM-20-74-4 (3 April 1974, E-PM) — Shore ice had been reduced to isolated patches of ice nearly black in color due to the presence of heavy minerals in the lag deposits.

49. CM-20-74-16 (6 April 1974, E-AM) — No ice was present at the study site.

APPENDIX C. SOURCES OF POSSIBLE ERRORS IN THE PHOTOGRAPHIC ANALYSIS

We utilized a high oblique photographic method to monitor the ice conditions along the shoreline of Lake Michigan. This method, like most, has limitations on the accuracy of the numbers that one obtains. This appendix describes and where possible quantifies errors that were encountered in the analysis. The errors recognized and discussed independently below are: slide remounting; marking the location of points on the projected picture; computer plotting; approximation of variable positions by a straight line; measurement of distances on the plots and position of the apparent horizon in the projected picture.

SLIDE REMOUNTING

For analysis each slide was removed from the original cardboard mount and was remounted on a 2 inch plexiglass square. Alignment of the sprocket holes in the color transparency with the guide lines on the plexiglass mount was only as accurate as the analyst's eye. Alignment with a given guide line was accurate within the width of that guide line (≈0.001"); hence, this source of error was negligible.

The overall position of the color transparency on the plastic mount was also checked. Before the oblique coordinates were assigned to data points on the projected image, the position of the photograph's projected principal point was verified. If the color transparency had been aligned either too high or too low on the plastic mount, the position of the principal point was corrected. Typical values for principal point displacement ranged from 0.10" to 0.20" in the projected image.

In order to evaluate the possible error in computed ground coordinates resulting from a displaced principal point, one slide was analyzed twice. The data for the slide were run first without the position of the principal point corrected and subsequently with the position correction. The results of the comparison indicated that the small errors in principal point location encountered in the study produced differences in the computed ground coordinates not exceeding 0.03 m.

MARKING POINTS ON THE PROJECTED PICTURE

The computer program utilizes the MSWL as the datum in its distance computations. Accurate calculations of ground distances required that the points denoting the positions of variables in the oblique image be marked where their intersection with the water surface was evident. In this study camera angles with respect to the true horizontal were very small and slight variation in the camera tilt angle would produce a large change in horizontal distance. The small camera depression angle introduced large displacement errors if points locating variable positions were marked on the projected photo above the apparent MSWL. The magnitude of the error in the computed ground distance to the variable was a function of the height of the variable above the MSWL and the distance of the variable from the camera, both of which determine the tilt and depression angles.

The relief error (Δx) was calculated for distances from the camera ranging from 60 m to 300 m and object heights up to 2 m. These values were decided upon as limits since heights calculated in the program never exceeded 2 m and ice structures were never nearer the camera than 60 m (in the direction of the camera's line-of-sight). Variables located near 300 m were isolated ice blocks and their intersection with the MSWL was easily observable in the projected photo thus reducing error in determining their locations.

The calculated relief correction values (Δx) have been displayed graphically allowing interpolation and rapid determination of variable displacement due to elevation above the datum.

We originally intended to calculate the possible displacement errors for each month's MSWL separately using the MSWL for the specific month. Figure 14 was based on the MSWL for February 1974. Calculations based on the MSWL for January 1974 showed deviations from the February values were limited to the second decimal place for the majority of cases, hence the February values were considered representative. The MSWL for the month was calculated by taking the average of the MSWL values at both Holland, Michigan and Calumet Harbor, Illinois.

The displacement error due to relief (Δx) is in the lakeward direction when ground distance values have been determined from oblique coordinates located above the MSWL datum. To avoid large relief errors, ice ridge positions were determined at the time of breakup when the intersection of the ice ridge with the water surface was evident.

COMPUTER PLOTTING

The printer plot subroutines called in the main program constructed two cartesian coordinate grids each with a different scale. One grid was scaled x = y = 1 inch : 150 ft, and the one used in the analysis, Figure 13, was scaled x = 1 inch : 100 ft and y = 1 inch : 150 ft.

On the plot used here 10 characters were plotted per inch representing 100 ft along the abscissa resulting in a plotting error of ±5 ft. Along the ordinate 24 plotted characters represented 600 ft, hence the maximum plotting error in the y direction was ±12.5 ft. Distance measurements made along the normal to the baseline had a possible error of $\pm\text{SQRT}\ (x^2_{\text{error}} + y^2_{\text{error}}) = \pm\text{SQRT}\ 5.0^2 + 12.5^2) = \pm 13.5$ ft.

APPROXIMATION OF VARIABLE POSITIONS BY STRAIGHT LINES

The variables were located on the plots in linear arrays that displayed a certain degree of scatter about the constructed line representing the average position. The points that located the position of the seawall showed the least scatter whereas those which located the breaker zones varied the furthest from the average line. The points that showed the position of the shore or the ice ridges were usually scattered less than those of the breaker zones. The scatter of the ground coordinate points from the constructed straight line had

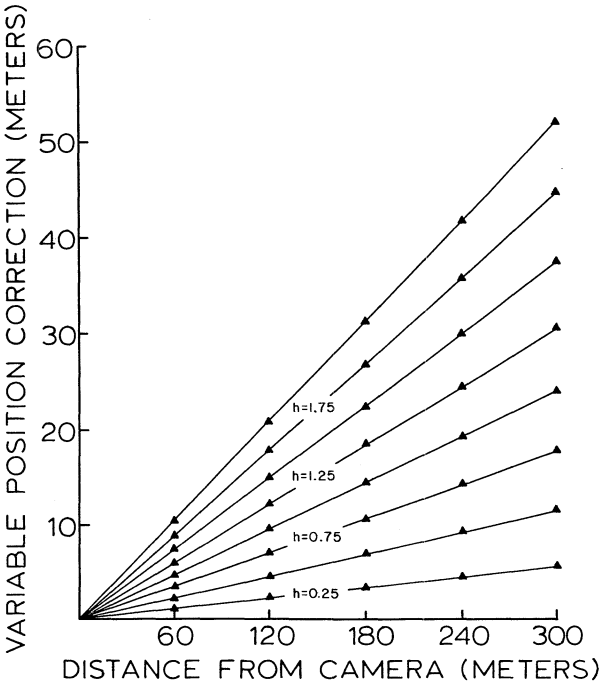

FIG. 14. Correction for relief error.

its origin from three sources, the variation incurred in plotting, the natural irregularity in the structure itself and the location of the constructed line of approximation.

It was difficult to assign a value to the error incurred by the straight line approximation without resorting to statistical methods. Any error that did exist was consistent throughout the entire study since all analyses were performed by one person. His reasoning for the line placement did not vary between cases. We suspect that a variation of 10 to 20 ft was present in some cases, but this variation applied to only one or two points along a line whose position was represented by six or more points. This was particularly true of the breaker zones where points were chosen only where the breaker was evident in the picture. As one might suspect, breakers are rarely continuous, and breaker zones are marked by a series of breaking waves.

A regression analysis was later performed on several data sets and the correlation coefficients ranged from 0.9 to 1.0 indicating the arrays of ground coordinate points (Fig. 13) could be accurately approximated with a straight line.

MEASUREMENT OF DISTANCES ON COMPUTER PLOTS

Appendix D explains how the distances from the baseline to the lines approximating variable locations were measured. The x and y components of the baseline normal were determined for each distance measurement. All measurements of distance on the computer plots were made with a dial caliper accurate to 0.001". For the plotting grid used in the analysis the maximum error in measurement in the y direction was 0.001 inch $*$ $\frac{150 \text{ feet}}{\text{inch}}$ or 0.150 ft. In the x direction the maximum error was 0.001 inch $*$ $\frac{100 \text{ feet}}{\text{inch}}$ or 0.100 ft.

ERROR RESULTING FROM OBSCURED HORIZON

Since slide CM-10-74-18 had a particularly clear horizon, it was selected as the control for evaluation of error in computed ground coordinate values resulting from an obscured horizon in the oblique photograph. The distance (PTSCRN) measured on the screen between the principal point of the projected oblique photograph and the image of the apparent horizon is used by ICESTUDY in the preliminary calculations for the equivalent vertical photograph. Any discrepancies in this measurement resulting from an obscured horizon will introduce error in the values computed for the principal plane diagram (Fig. 2) and subsequent ground coordinate values.

Increments of ±0.10" were added and subtracted from the control value for PTSCRN used in the analysis of slide CM-10-74-18. These plus and minus increments represented the possible errors in selection of the location of the apparent horizon in a projected oblique photograph with an obscured horizon. We are confident that errors in selecting the position of the apparent horizon in the oblique representation never exceeded 0.15 inches. This corresponds to a negligible error in the x ground coordinate of less than one foot and less

than 8 ft in the y ground coordinate direction. Only 4% to 5% of the slides analyzed could conceivably involve errors of this magnitude. When this condition was encountered the selected horizon location was compared with an average value for PTSCRN as well as with that for both the preceding and following slides to minimize this source of error.

APPENDIX D. METHOD USED IN THE DETERMINATION OF MONITORED VARIABLE POSITIONS

The discussion presented here is the method used in determining the location of the monitored variable positions. Figure 15 is used as a basis for reference in the discussion.

1. Construct the baseline (A) through the asterisks which represent the location of the seawall. The asterisk located at (57.0, 1247.0) represents the position of the north rangepole.

2. The location of other variable positions on the plot may be approximated by lines B, C, D drawn through the plotted characters locating each variable.

(O) = runups (Line B)

(·) = ice ridge or boundary (Line C)

(X) = breaker zones (Line D)

3. Construct the normal (EH) to the baseline (Line A) at point (E).

4. Points F, G, H are formed by the intersection of the baseline normal and the lines B, C, and D locating the positions of the other variables on the plot. From these points of intersection (F, G, H) construct lines HK, GJ, and FI parallel to the ordinate of sufficient length to intersect a line drawn through point E that is parallel to the abscissa, in this case the horizontal printer plot grid line.

5. Determine the lengths of the X and Y components of the resulting right triangle. Ground distances EF, EG, and EH, measured from the baseline, can be computed by application of the plotting scale and the Pythagorean Theorem.

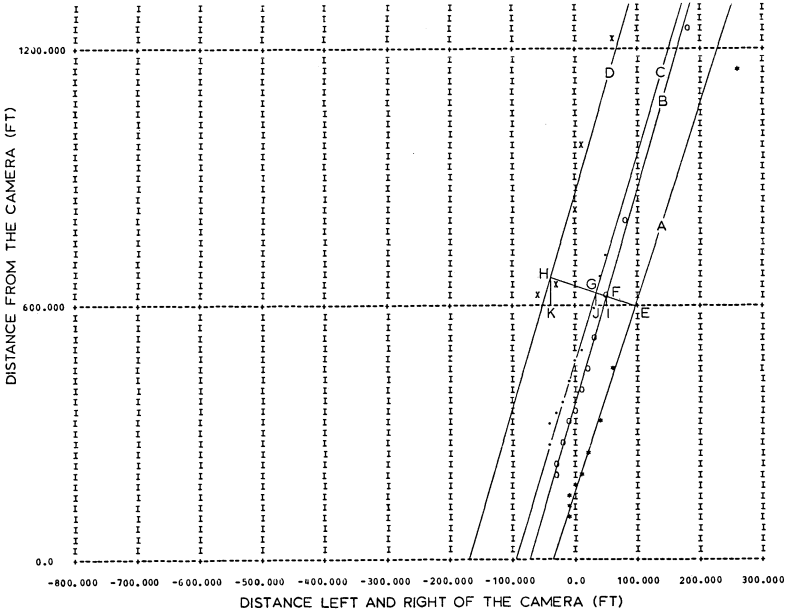

FIG. 15. Sample line printer plot and graphic techniques.

APPENDIX E. COMPUTER PROGRAM *ICESTUDY*

```
C     THE OBJECTIVE OF THIS PROGRAM IS TO DETERMINE GROUND COORDINATES
C     OF ICE RIDGES, BREAKER ZONES AND RRASH ICE ZONES. THE HEIGHTS OF
C     ICE STRUCTURES AND THE AREAS OF ICE ACCUMULATIONS FROM HIGH
C     OBLIQUE PHOTOGRAPHS PROJECTED ON A SCREEN THROUGH A SLIDE
C     PROJECTOR.
C
C     THE VARIABLES USED IN THE PROGRAM:
C
C     TAIR=TEMPERATURE OF THE AIR
C     TH2O=TEMPERATURE OF THE SURFACE WATER
C     TAIR, TH2O ARE READ IN DEGREES F AND CONVERTED INTO DEGREES C
C     STICE=ICE CONDITION INDEX - R-UP=BREAKUP, DETR=DETERIORATION
C     STAT=STATIC, ACCR=ACCRETION, NONE=NO ICE PRESENT
C     SLTR=PERPENDICULAR DISTANCE THROUGH THE PRINCIPAL POINT BETWEEN
C     A HORIZONTAL LINE AT THE TOP OF THE PLASTIC MOUNT AND A
C     HORIZONTAL LINE AT THE BOTTOM OF THE PLASTIC MOUNT
C     SCTR=PERPENDICULAR DISTANCE MEASURED ON SCREEN BETWEEN
C     THE IMAGES OF THE SAME LINES USED IN CALCULATING SLTR
C     SLIDE=ONE HALF THE DISTANCE MEASURED ON THE SLIDE (0.5*SLTR)
C     SCREEN=ONE HALF THE DISTANCE MEASURED ON THE SCREEN (0.5*SCTR)
C     FPROJ=FOCAL LENGTH OF THE SLIDE PROJECTOR
C     FCAM=FOCAL LENGTH OF THE CAMERA LENS = 50MM OR 1.97 INCHES
C     PTSCRN=DISTANCE PT MEASURED ON THE SCREEN, DISTANCE FROM PRINCIPAL
C        POINT TO APPARENT HORIZON.
C     H=HEIGHT ABOVE THE MEAN STILL WATER LEVEL.
C     SWL=MEAN STILL WATER LEVEL
C     ILENS=DISTANCE FROM LENS TO SLIDE IN THE PROJECTOR, CALCULATED
C     USING SIMILAR TRIANGLES AND THE GAUSSIAN FORM OF THE THIN LENS
C     EQUATION
C     HORIZ= HORIZON INDEX. 1=EXCELLENT, 2=GOOD, 3=FAIR, 4=POOR
C     DIP=DIP ANGLE, ANGLE FROM TRUE HORIZON TO APPARENT HORIZON.
C     THETA=DEPRESSION ANGLE.
C     T=TILT ANGLE OR 90-THETA
C     PT.PI.TN.IN.TI=DISTANCES ON THE PRINCIPAL PLANE DIAGRAM.
C     RFI=FCAM/H
C     D=DISTANCE FROM PROJECTOR LENS TO SCREEN.
C     GI=1/RFI
C     XRUNY().YRUNY()=COORDINATES OF THE REFERENCE POINTS COMMON TO ALL
C     SLIDES
C     XBZONE().YBZONE()=COORDINATES OF THE BREAKER ZONES
C     XRUNUP().YRUNUP()=COORDINATES OF THE RUNUPS
C     XRIDGE().YRIDGE()=COORDINATES OF THE ICE RIDGES
C     XBGYGD().YBGYGD()=REAL GROUND COORDINATES OF THE REFERENCE POINTS
C     COMMON TO ALL SLIDES
C     XBZGD().YBZGD=REAL GROUND COORDINATES OF THE BREAKER ZONES
C     XRUNGD().YRUNGD()=REAL GROUND COORDINATES OF THE RUNUPS
C     XRIGD().YRIGD()=REAL GROUND COORDINATES OF THE ICE RIDGES
C     XICE().YICE()=COORDINATES DEFINING THE AREAS OF ICE ACCUMULATION
C     XICEGD().YICEGD()=REAL GROUND COORDINATES OF THE OUTLINE OF THE
C     ICE ACCUMULATIONS
C     AREA()=AREA OF THE ICE ACCUMULATIONS AT TIMDAY CALCULATED BY THE
C     COORDINATE METHOD UNITS=SQUARE FEET
C     ARSM=AREA IN SQUARE METERS
C     AX,AY=POINT PICKED OFF PHOTOGRAPH AT PEAK OF OBJECT WHOSE HEIGHT
C     IS BEING CALCULATED-USED IN CALCULATING THE EQUIVALENT VERTICAL
C     PHOTO COORDINATES OF POINT AY
C     BX,BY=POINT DIRECTLY BENEATH POINT AX,AY
C     T1=TANGENT OF ANGLE THETA=TANGENT OF ANGLE TO POINT AX,AY
C     LF=DA=DISTANCE FROM CAMERA TO AX,AY
```

```
C      CB=DISTANCE FROM CAMERA TO BX,BX
C      TIMDAY=THE TIME OF DAY IN CATEGORIES E-AM, L-AM, NOON, E-PM, L-PM
C      D IS D PRIMED IN THE VERTICAL HEIGHT FORMULA
C      R IS R PRIMED IN THE VERTICAL HEIGHT FORMULA
C      TS IS THE DISTANCE TS IN THE VERTICAL HEIGHT FORMUA
C      IF ANY OF THE K'S ARE 0, THERE IS NO INPUT FOR THAT PARAMETER
C      K1=NUMBER OF PHOTO REFERENCE POINTS (NUMBER OF XBUOY(),YBUOY()
C      PAIRS INPUTED PER SLIDE)
C      K2=NUMBER OF XBZONE(),YBZONE() PAIRS
C      K3=NUMBER OF XRUNUP(),YRUNUP() PAIRS
C      K4=NUMBER OF XRIDGE(),YRIDGE() PAIRS
C      K7=NUMBER OF ICE ACCUMULATION AREAS ANALYZED PER SEQUENCE
C      K8=NUMBER OF XICE(),YICE() PAIRS PER ICE ACCUMULATION
C      K9=NUMBER OF 'BY' POINTS PICKED TO USE IN THE ITERATION
C      K10=NUMBER OF SLIDES ANALYZED IN THIS RUN
C      K15=NUMBER OF POINTS DEFINING SEAWALL LOCATION
C      K16=K15+1=LAST X,Y BUOY POINT TO BE ENTERED IN THAT DATA SEGMENT
C      THIS LAST POINT LOCATES THE RANGE POLE
C      H1=HEIGHT OF CAMERA ABOVE SEAWALL
C      H2=HEIGHT OF CAMERA ABOVE REFERENCE POINT ON RANGE POLE
C
C
C      THE PROGRAM THAT FOLLOWS=OBLIQUE PHOTOGRAPHIC INTERPRETATION
C
C      THE FOLLOWING DEFINES AND DIMENSIONALIZES THE VARIABLES
C
       INTEGER MONTH,DAY,YEAR,PICT(3)
       INTEGER HORIZN,TIMDAY
       REAL ILENS,IN
       DIMENSION XBUOY(50),YBUOY(50),XBOYGD(50),YBOYGD(50)
       DIMENSION XBZONE(50),YBZONE(50),XBZGD(50),YBZGD(50),G2(50)
       DIMENSION XRUNUP(50),YRUNUP(50),XRUNGD(50),YRUNGD(50)
       DIMENSION XRIDGE(50),YRIDGE(50),XRIDGD(50),YRIDGD(50)
       DIMENSION XICE(50),YICE(50),XICEGD(50),YICEGD(50)
       DIMENSION A(50),AREA(50),AREAM(50)
       LOGICAL*1 BCD(4)/'*','X','O',' '/
       DIMENSION IMAGE (6200),X(100),Y(100)
       INTEGER CNT1/0/,CNT2/0/,CNT3/0/,CNT4/0/
       DIMENSION X1(2000),Y1(2000),X2(2000),Y2(2000),X3(2000),Y3(2000),X4
      1(2000),Y4(2000)
       DIMENSION Z1(2000),W1(2000),Z2(2000),W2(2000),Z3(2000),W3(2000),Z4
      1(2000),W4(2000)
C
C      THE OBJECTIVE OF THIS PART OF THE PROGRAM IS TO DETERMINE DISTANCES
C         ON THE PRINCIPAL PLANE DIAGRAM.
C
C      INPUT THE NUMBER OF SLIDES ANALYZED IN THIS RUN
       READ(5,1000) K10
       IKOUNT=0
 0200  IKOUNT=IKOUNT+1
C      INPUT DATE, SLIDE NUMBER, AIR AND H2O TEMPERATURES AND ICE COND.
       READ (5,901)MONTH,DAY,YEAR,PICT(1),PICT(2),PICT(3),TAIR,TH2O,
      1STICE
  901  FORMAT(2I3,I5,4X,3A4,2F10.2,A4)
C      CONVERT TAIR AND TH2O FROM DEGREES F TO DEGREES C
       TAIR=(TAIR-32.0)*0.5556
       TH2O=(TH2O-32.0)*0.5556
       WRITE (6,902)MONTH,DAY,YEAR,PICT(1),PICT(2),PICT(3),TAIR,TH2O,
      1STICE
  902  FORMAT('-',25X,3I8,5X,3A4,2F10.2,5X,A4)
```

```
      READ (5,900) FCAM
      READ(5,905) SWL,PTSCRN
C
C     CALCULATE FOCAL LENGTH OF THE PROJECTOR
C
      READ (5,906) SLTR,SCTR
      SLIDE = SLTR/2.0
      SCREEN = SCTR/2.0
      D = 92.0*SCREEN/(SLIDE+SCREEN)
      ALPHA = 92.0-D
      FPROJ = ALPHA*D/(ALPHA+D)
      READ(5,910) HORIZN,TIMDAY
      ILENS=(D*FPROJ)/(D-FPROJ)
      C=ILENS/D
      WRITE(6,800)FCAM,FPROJ,D,SWL,PTSCRN,HORIZN,TIMDAY
      WRITE(6,805)ILENS,C
C
C     CALCULATE DISTANCES ON THE PRINCIPAL PLANE DIAGRAM
C
      PT=PTSCRN*C
      V=PT/FCAM
      H=(624.546-SWL)
      DIP=0.98*SQRT(H)
      ANGLE=V
      THETA1=ATAN(ANGLE)/(2.0*3.14159/360.0000)
      THETA=((DIP/60.0000)+THETA1)*(2.0*3.14159/360.0000)
      PT=TAN(THETA)*FCAM
      THETA=THETA/(2.0*3.14159/360.0000)
      T=(90.0000-THETA)*(2.0*3.14159/360.0000)
      TT=0.5*T
      PN=FCAM*TAN(T)
      PI=FCAM*TAN(TT)
      TI=PT+PI
      TN=PN+PT
      IN=TN-TI
      T=T/(2.0*3.14159/360.0000)
      WRITE(6,810)DIP,THETA1,THETA,T,TN,TI,PT,PI,IN
C
C     THE OBJECTIVE OF THIS PART OF THE PROGRAM
C     IS TO DETERMINE HORIZONTAL DISTANCES
C
C
C     IN EACH CASE THE COORDINATES OF THE POINTS ARE FIRST CALCULATED
C     FOR THE EQUIVALENT VERTICAL PHOTOGRAPH (COORDINATE AXES ORIGIN
C     AT ISOCENTER) AND THEN THE REAL GROUND COORDINATES (COORDINATE
C     AXES ORIGIN AT CAMERA) ARE CALCULATED
C
C     INPUT XBUOY(),YBUOY(),K1,K15,K16 AND CALCULATE GROUND COORDINATES
C     FOR THE REFERENCE POINTS
C
      READ (5,915)K1,K15,K16
      IF(K1.EQ.0) GO TO 100
      H1=38.63
      H2=15.17
      DO 1 I=1,K1
      READ(5,920) XBUOY(I),YBUOY(I)
 0001 CONTINUE
      WRITE(6,820)
 0820 FORMAT('  XBUOY(I)   YBUOY(I)   I    K1')
      DO 2 I=1,K1
```

```
      WRITE(6,825) XBUOY(I),YBUOY(I),I,K1
 0002 CONTINUE
      DO 3 I=1,K1
      IF (I.GT.0.AND.I.LE.K15) H=H1
      IF (I.GT.K15.AND.I.LE.K16) H=H2
      G1=YBUOY(I)*C+PI
      YBUOY(I)=G1*(TI/(TI-G1))
      XBUOY(I)=XBUOY(I)*C*(TI/(TI-G1))
      YBOYGD(I)=(H*(PI+YBUOY(I)))/FCAM
      XBOYGD(I)=H*XBUOY(I)/FCAM
 0003 CONTINUE
      H= (624.546-SWL)
      WRITE(6,830)
 0830 FORMAT( ' I  XBUOY(I)  YBUOY(I)  XBOYGD(I) YBOYGD(I)')
      DO 4 I=1,K1
      WRITE(6,835)I,XBUOY(I),YBUOY(I),XBOYGD(I),YBOYGD(I)
 0004 CONTINUE
C
C     INPUT XRZONE(),YRZONE(),K2, AND CALCULATE THE GROUND COORDINATES
C     FOR THE BREAKER ZONES
C
 0100 READ(5,925)K2
      IF(K2.EQ.0) GO TO 110
      WRITE(6,840)
 0840 FORMAT( ' I  XRZONE(I) YRZONE(I) K2 ')
      DO 11 I=1,K2
      READ(5,930) XRZONE(I),YRZONE(I)
      WRITE(6,845)I,XRZONE(I),YRZONE(I),K2
 0011 CONTINUE
      DO 12 I=1,K2
      G2(I)=YRZONE(I)*C+PI
      YRZONE(I)=G2(I)*(TI/(TI-G2(I)))
      XRZONE(I)=XRZONE(I)*C*(TI/(TI-G2(I)))
      YRZGD(I)=(H*(PI+YRZONE(I)))/FCAM
      XRZGD(I)=H*XRZONE(I)/FCAM
 0012 CONTINUE
      WRITE(6,850)
 0850 FORMAT(3X,'I XRZONE(I) YRZONE(I) XRZGD(I) YRZGD(I)      G2(I)')
      DO 13 I=1,K2
      WRITE(6,855)I,XRZONE(I),YRZONE(I),XRZGD(I),YRZGD(I),G2(I)
 0013 CONTINUE
C
C      INPUT XRUNUP(),YRUNUP(),K3, AND CALCULATE THE GROUND COORDINATES
C     FOR THE RUNUPS
C
 0110 READ(5,935)K3
      IF(K3.EQ.0) GO TO 120
      WRITE(6,860)
 0860 FORMAT( ' I  XRUNUP(I) YRUNUP(I) K3 ')
      DO 20 I=1,K3
      READ(5,940) XRUNUP(I),YRUNUP(I)
      WRITE(6,865)I,XRUNUP(I),YRUNUP(I),K3
 0020 CONTINUE
      WRITE(6,870)
 0870 FORMAT( ' I  XRUNUP(I) YRUNUP(I) XRUNGD(I) YRUNGD(I) ')
      DO 21 I=1,K3
      G3=YRUNUP(I)*C+PI
      YRUNUP(I)=G3*(TI/(TI-G3))
      XRUNUP(I)=XRUNUP(I)*C*(TI/(TI-G3))
      YRUNGD(I)=(H*(PI+YRUNUP(I)))/FCAM
```

```
      XRUNGD(I)=H*XRUNUP(I)/FCAM
      WRITE(6,875)I,XRUNUP(I),YRUNUP(I),XRUNGD(I),YRUNGD(I)
 0021 CONTINUE
C
C     INPUT XRIDGE(),YRIDGE(),K4, AND CALCULATE THE GROUND COORDINATES
C     FOR THE ICE RIDGES
C
 0120 READ(5,945) K4
      IF(K4.EQ.0) GO TO 130
      WRITE(6,890)
 0890 FORMAT( '   I   XRIDGE(I),YRIDGE(I) K4 ')
      DO 30 I=1,K4
      READ(5,950)XRIDGE(I),YRIDGE(I)
      WRITE(6,885)I,XRIDGE(I),YRIDGE(I),K4
 0030 CONTINUE
      WRITE(6,880)
 0880 FORMAT( '   I   XRIDGE(I) YRIDGE(I) XRIDGD(I) YRIDGD(I)  ')
      DO 31 I=1,K4
      G4=YRIDGE(I)*C+PI
      YRIDGE(I)=G4*(TI/(TI-G4))
      XRIDGE(I)=XRIDGE(I)*C*(TI/(TI-G4))
      YRIDGD(I)=(H*(PI+YRIDGE(I)))/FCAM
      XRIDGD(I)=H*XRIDGE(I)/FCAM
      WRITE(6,895)I,XRIDGE(I),YRIDGE(I),XRIDGD(I),YRIDGD(I)
 0031 CONTINUE
 0130 CONTINUE
      WRITE(6,4870)
 4870 FORMAT ( 1H1)
      ISUM=1
      KNT1=0
      KNT2=0
      KNT3=0
      KNT4=0
C     SET UP INFORMATION REQUIRED TO CONSTRUCT THE PLOT
      CALL PLOT1 (0.,6.,23.,12.,9)
C     PREPARE GRID AND SET UP INFORMATION REQUIRED BY PLOT3 TO
C     PLACE POINT IN GRAPH
      CALL PLOT2 (0.,300.0,-800.0,3000.0,0.0)
      IF (K1 .EQ. 0) GO TO 4876
      DO 4871 I=1,K1
      CNT1 = CNT1+1
      KNT1 = KNT1+1
      X(I)=XRDYGD (I)
      XI(CNT1)=X(I)
      ZI(KNT1)=X(I)
      Y(I)=YRDYGD (I)
      YI(CNT1)=Y(I)
      W1(KNT1)=Y(I)
C     PLACE PLOTTING CHARACTER IN THE GRAPH FOR EACH (X,Y)
C     COORDINATE POINT
      CALL PLOT3(BCD(1),X(I),Y(I),1.4)
 4871 CONTINUE
 4876 CONTINUE
      ISUM=ISUM +K1
      IF (K2 .EQ. 0) GO TO 4877
      IS=K1+K2
      DO 4872 I=ISUM.IS
      CNT2 = CNT2+1
      KNT2=KNT2+1
      X(I)=XRZGD(I-K1)
```

```
      X2(CNT2)=X(I)
      Z2(KNT2)=X(I)
      Y(I)=YRZGD(I-K1)
      Y2(CNT2)=Y(I)
      W2(KNT2)=Y(I)
      CALL PLOT3 (RCD(2),X(I),Y(I),1.4)
 4872 CONTINUE
 4877 CONTINUE
      ISUM=ISUM+K2
      IF (K3 .EQ. 0) GO TO 4878
      IS=K1+K2+K3
      DO 4873 I=ISUM,IS
      CNT3 = CNT3+1
      KNT3=KNT3+1
      X(I)=XRUNGD(I-K1-K2)
      X3(CNT3)=X(I)
      Z3(KNT3)=X(I)
      Y(I)=YRUNGD(I-K1-K2)
      Y3(CNT3)=Y(I)
      W3(KNT3)=Y(I)
      CALL PLOT3 (RCD(3),X(I),Y(I),1.4)
 4873 CONTINUE
 4878 CONTINUE
      ISUM=ISUM +K3
      IF (K4 .EQ. 0) GO TO 4879
      IS=K1+K2+K3+K4
      DO 4874 I=ISUM,IS
      CNT4 = CNT4+1
      KNT4=KNT4+1
      X(I)=YRINGD(I-K1-K2-K3)
      X4(CNT4)=X(I)
      Z4(KNT4)=X(I)
      Y(I)=YKINGD(I-K1-K2-K3)
      Y4(CNT4)=Y(I)
      W4(KNT4)=Y(I)
      CALL PLOT3 (RCD(4),X(I),Y(I),1.4)
 4874 CONTINUE
 4879 CONTINUE
C     PRINT THE COMPLETED GRAPH AND LABEL
      CALL PLOT4 (20,'DISTANCE FROM CAMERA')
      WRITE (6,4891)
 4891 FORMAT (1H0,50X,'DISTANCE LEFT AND RIGHT OF THE CAMERA')
      WRITE (6,5555)
      CALL PLOT1 (0.6,23.12.9)
      CALL PLOT2(0.600,0.-1050.0,3000.0,0.0)
      CALL PLOT3 (RCD(1),Z1,W1,KNT1,4)
      CALL PLOT3 (RCD(2),Z2,W2,KNT2,4)
      CALL PLOT3 (RCD(3),Z3,W3,KNT3,4)
      CALL PLOT3 (RCD(4),Z4,W4,KNT4,4)
      CALL PLOT4 (20,'DISTANCE FROM CAMERA')
      WRITE(6,4891)
C
C     THE PURPOSE OF THIS SECTION OF THE PROGRAM IS TO CALCULATE
C     THE AREA OF ICE ACCUMULATIONS
C
C     INPUT XICE(),YICE(),TIMDAY,K7,K8
C
      READ(5,970) K7
      IF(K7.EQ.0) GO TO 160
      WRITE(6,730)
```

```
 0730 FORMAT('    I     J     TIMDAY        XICE(J)      YICE(J)      K7
     1K8')
      DO 60 I=1,K7
      READ(5,975)K8,TIMDAY
      DO 61 J=1,K8
      READ(5,980)XICE(J),YICE(J)
      WRITE(6,735) I,J,TIMDAY,XICE(J),YICE(J),K7,K8
 0061 CONTINUE
      WRITE(6,740)
  740 FORMAT('    I     J     XICE(J)      YICE(J)    XICEGD(J)    YICEGD(J)
     1')
      DO 62 J=1,K8
      G6=YICE(J)*C+PI
      YICE(J)=G6*(TI/(TI-G6))
      XICE(J)=XICE(J)*C*(TI/(TI-G6))
      YICEGD(J)=(H*(PI+YICE(J)))/FCAM
      XICEGD(J)=H*XICE(J)/FCAM
      WRITE(6,745)I,J,XICE(J),YICE(J),XICEGD(J),YICEGD(J)
 0062 CONTINUE
      AREA(1)=0.0
      AREA(2)=0.0
      N3=K8-1
      DO 63 J=1,N3
      A(J+1)=((XICEGD(J)+XICEGD(J+1))*0.50)*(YICEGD(J)-YICEGD(J+1))
      AREA(J+1)=AREA(J)+A(J+1)
 0063 CONTINUE
 0161 AREA(I)=AREA(K8)-((XICEGD(1)+XICEGD(K8)) *0.5)*(YICEGD(1)-YICEGD(K
     18))
C
C     CONVERT AREA(I)(SQUARE FEET) INTO SQUARE METERS
C
      AREAM(I)=AREA(I)*0.0929
      WRITE(6,750)I,AREA(I),I,AREAM(I)
 0060 CONTINUE
  160 CONTINUE
C
C     THIS SECTION OF THE PROGRAM CALCULATES HEIGHTS
C
C     INPUT K9 AND THE PAIRS OF COORDINATE POINTS FOR
C     THE HEIGHT CALCULATION
C
      READ(5,912)K9
 0912 FORMAT(I4)
      IF(K9.EQ.0) GO TO 170
      DO 4444 II=1,K9
      READ(5,987)AX,AY,BX,BY
  987 FORMAT (4F10.3)
      G7=PI+C*AY
      YAY=G7*(TI/(TI-G7))
      XAX=AX*C*(TI/(TI-G7))
      G8=PI+C*BY
      YBY=G8*(TI/(TI-G8))
      XBX=BX*C*(TI/(TI-G8))
      D=G7-G8
      R=IN+G7
      TS=TI-G8
      HTR=H*((D*TN)/(R*TS))
      WRITE(6,956)G7,G8,D,TS,R,H,TN,HTR
  956 FORMAT (1X,8F10.4)
      YAYGD=((H-0.5*HTR)*(PI+YBY))/FCAM
```

```
      XAXGD=H*XAX/FCAM
C     CONVERT HEIGHT(HTR) FROM FEET TO METERS
      HTRM=HTR*0.3048
      WRITE(6,5080)
 5080 FORMAT(8X'XAXGD          YAYGD     IKOUNT          HTR          HTBM')
      WRITE(6,5081)XAXGD,YAYGD,IKOUNT,HTR,HTBM
 5081 FORMAT(4X,F10.3,2X,F10.3,5X,I3,5X,F10.3,2X,F10.3)
 4444 CONTINUE
 0170 IF(IKOUNT.LT.K10) GO TO 200
 0771 CONTINUE
      WRITE (6,5555)
 5555 FORMAT (1H1)
C
C     THE PLOTS CALLED HERE ARE CUMULATIVE FOR ALL SLIDES ANALYZED
C     IN THIS RUN
C
      CALL PLOT1 (0.,6.23,12,9)
      CALL PLOT2 (0.300.0,-800.0,3000.0,0.0)
      CALL PLOT3 (RCD(1),X1,Y1,CNT1,4)
      CALL PLOT3 (RCD(2),X2,Y2,CNT2,4)
      CALL PLOT3 (RCD(3),X3,Y3,CNT3,4)
      CALL PLOT3 (RCD(4),X4,Y4,CNT4,4)
      CALL PLOT4 (20,'DISTANCE FROM CAMERA')
      WRITE(6,4891)
      WRITE (6,5555)
      CALL PLOT1 (0.,6.23,12,9)
      CALL PLOT2(0.600.0,-1050.0,3000.0,0.0)
      CALL PLOT3 (RCD(1),X1,Y1,CNT1,4)
      CALL PLOT3 (RCD(2),X2,Y2,CNT2,4)
      CALL PLOT3 (RCD(3),X3,Y3,CNT3,4)
      CALL PLOT3 (RCD(4),X4,Y4,CNT4,4)
      CALL PLOT4 (20,'DISTANCE FROM CAMERA')
      WRITE(6,4891)
 1000 FORMAT(I4)
  900 FORMAT (F10.4)
 0905 FORMAT(2F10.3)
  906 FORMAT (2F10.3)
  910 FORMAT(I1,A4)
 0915 FORMAT (3I4)
 0920 FORMAT(2F10.3)
 0925 FORMAT(I4)
 0930 FORMAT(2F10.3)
 0935 FORMAT(I4)
 0940 FORMAT(2F10.3)
 0945 FORMAT(I4)
 0950 FORMAT(2F10.3)
 0955 FORMAT(I4)
 0960 FORMAT(I4)
 0965 FORMAT(2F10.3)
 0970 FORMAT(I4)
  975 FORMAT(I4,A4)
 0980 FORMAT(2F10.3)
 0985 FORMAT(I4,2F10.3)
 0990 FORMAT(2F10.3)
 0995 FORMAT(F10.3)
  800 FORMAT('-',5F10.3,I5,4X,A4)
  805 FORMAT(2F10.3)
 0810 FORMAT(9F10.3)
 0825 FORMAT(2F10.3,2I4)
 0835 FORMAT(I4,4F10.3)
```

```
 0845 FORMAT(I4,2F10.3,I4)
 0855 FORMAT(I4,5F10.3)
 0865 FORMAT(I4,2F10.3,I4)
 0875 FORMAT(I4,4F10.3)
 0885 FORMAT(I4,2F10.3,I4)
 0895 FORMAT(I4,4F10.3)
 0705 FORMAT(2I4,2F10.3,2I4)
 0715 FORMAT(2I4,4F10.3)
 0720 FORMAT(F10.4,4I10)
 0725 FORMAT(4F10.4,2I4)
  735 FORMAT(2I5.5X.A4.5X.F10.3,2X,F10.3,2X,I5,2X,I5)
  745 FORMAT (2I5,2X,F10.3,2X,F10.3,2X,F10.3,2X,F10.3)
  750 FORMAT('AREA(',I3,')=',E20.2,5X,'AREAM(',I3,')=',E20.2)
 0755 FORMAT(4F10.3)
 0760 FORMAT(2F10.3)
 0770 FORMAT(2F10.3)
      STOP
      END
$ENDFILE
$SIG
                                                        500  LINES PRINTED
```

APPENDIX F. SUMMARY TABLE OF CLIMATIC VARIABLES: JANUARY AND FEBRUARY 1974

January 1974

Date	Wind direction				Wind speed (knots)			
	0200	0800	1400	2000	0200	0800	1400	2000
1	ESE	WNW	W	WSW	5	18	18	15
2	SSW	SE	ESE	ESE	5	8	5	7
3	E	E	ESE	WNW	6	6	5	18
4	W	W	W	SW	12	10	10	12
5	S	SE	SW	WSW	5	5	10	14
6	W	SSW	SW	WSW	8	10	16	14
7	WSW	WSW	W	W	20	24	18	17
8	SE	E	ESE	E	8	5	9	10
9	E	NE	E	ESE	5	6	5	5
10	ESE	E	NE	NE	5	8	10	5
11	NNE	NNE	NE	W	7	6	3	20
12	NW	WNW	WNW	WSW	20	24	12	16
13	SE	SE	SE	E	8	5	10	7
14	SE	SSW	SW	SSW	9	12	13	10
15	S	S	WNW	S	8	10	18	3
16	SW	SSW	SW	SW	10	14	13	6
17	W	ENE	ESE	E	5	12	12	15
18	E	ESE	ESE	NE	10	15	8	7
19	N	NE	NE	E	8	8	12	8
20	E	ESE	E	ESE	15	12	10	10
21	S	WSW	WSW	W	5	18	18	18
22	SSW	ESE	E	ESE	8	5	5	5
23	W	W	W	SW	10	25	16	18
24	SW	S	SSW	SW	5	5	8	14
25	SSW	S	SSW	S	6	8	8	4
26	ESE	ESE	SE	E	10	8	9	15
27	S	WSW	W	WSW	10	25	22	20
28	W	NE	E	NNW	2	4	5	8
29	WSW	SSW	SE	S	12	9	8	8
30	S	SSW	SSW	S	15	10	14	10
31	S	SW	NW	WNW	11	20	35	18

January 1974

Date	Air temperature °C 0200	0800	1400	2000	Ice cond. ~0800 E-AM	~1400 E-PM	Water temperature °C 0200	0800	1400	2000
1	-7.8	-8.3	-7.8	-12.2	*	*	1.7	1.7	1.7	1.7
2	-13.3	-13.9	-8.9	-10.0	*	*	1.7	1.7	1.7	1.7
3	-8.9	-8.9	-5.0	-4.4	*	*	1.7	1.7	1.1	1.1
4	-6.7	-7.8	4.4	-4.4	*	*	1.1	1.1	1.1	1.1
5	-9.4	-10.6	-3.3	-5.0	*	*	1.1	1.1	1.1	1.1
6	-4.4	-5.6	-4.4	-6.7	*	*	1.1	1.1	1.1	1.1
7	-6.7	-7.2	-7.8	-10.0	*	*	1.1	1.1	0.6	0.6
8	-13.3	-14.4	-8.9	-8.9	*	*	0.6	-0.6	-0.6	-0.6
9	-8.9	-11.1	-2.2	-5.0	*	*	-0.6	-0.6	-0.6	-0.6
10	-6.7	-7.8	-3.9	-6.7	*	*	-0.6	-0.6	1.1	1.1
11	-7.2	-7.2	5.6	-3.3	*	*	1.1	1.1	0.6	0.6
12	-7.8	-10.0	-7.8	-10.0	*	*	0.6	0.6	0.6	0.6
13	-17.8	-17.2	-10.0	-7.8	*	*	0.6	0.6	0.0	0.0
14	-5.6	-3.9	-1.1	0.6	*	*	0.0	0.0	1.1	1.1
15	-1.1	-1.1	6.7	0.6	*	*	1.1	1.1	1.1	1.1
16	-1.1	1.1	5.6	4.4	STAT	STAT	0.6	1.1	1.1	1.1
17	0.0	-2.2	-1.1	-1.1	B-UP	DETR	1.1	1.1	1.1	0.6
18	-2.2	-1.7	2.2	2.2	DETR	DETR	0.6	0.6	0.6	0.6
19	0.0	0.6	0.0	0.0	*	*	0.6	0.6	0.6	0.6
20	0.6	2.8	6.7	8.9	*	*	0.6	0.6	0.6	0.6
21	7.8	1.7	2.2	1.7	*	*	0.6	0.6	0.6	0.6
22	0.0	0.6	1.1	1.7	DETR	DETR	0.6	0.6	0.6	0.6
23	1.1	0.0	1.1	0.0	B-UP	B-UP	0.6	1.7	1.7	1.7
24	-1.7	-1.1	3.3	1.1	STAT	STAT	1.7	1.7	1.7	1.7
25	0.6	-0.6	10.0	4.4	ACCR	ACCR	1.7	1.7	1.7	1.7
26	2.2	0.0	5.6	6.7	DETR	STAT	1.7	1.7	1.7	1.7
27	3.3	2.8	1.1	1.1	B-UP	DETR	1.7	1.7	1.7	1.7
28	-1.1	-1.1	-1.1	-0.6	DETR	*	1.7	1.7	1.7	1.7
29	-0.6	-1.7	-1.1	-1.1	STAT	STAT	1.7	1.7	1.7	1.7
30	2.2	2.8	4.4	8.9	ACCR	STAT	1.7	1.7	1.7	1.7
31	7.2	3.3	3.3	-3.9	B-UP	NONE	1.7	1.7	1.7	1.7

*Missing data

February 1974

Date	Wind direction				Wind speed (knots)			
	0200	0800	1400	2000	0200	0800	1400	2000
1	NW	ENE	ENE	E	11	5	12	8
2	ENE	ENE	E	*	10	11	11	*
3	ENE	E	SSE	WNW	6	8	8	10
4	WNW	W	NNE	ESE	17	10	4	4
5	ESE	ESE	E	E	7	10	10	20
6	ENE	ENE	NE	NE	8	19	10	8
7	N	NE	NE	NE	10	5	10	5
8	E	SSE	W	*	6	3	14	*
9	W	W	E	WNW	15	15	5	15
10	S	S	NNW	NW	10	8	23	20
11	NW	*	SW	SSW	10	*	14	18
12	E	SE	SE	SSW	5	8	9	5
13	S	S	NNE	NNW	5	2	5	15
14	N	E	ENE	NNE	14	10	12	10
15	ENE	E	E	E	5	10	10	8
16	ESE	S	SW	NNW	5	4	15	6
17	W	NNW	W	NNE	5	10	8	7
18	E	ESE	SE	S	10	20	10	6
19	S	N	N	NNW	5	9	15	12
20	NW	SW	SSW	S	5	4	8	5
21	ESE	ESE	E	E	5	8	12	12
22	NE	E	NW	NW	14	8	25	25
23	NW	NW	NW	NNW	15	15	10	8
24	NE	NE	NE	NNW	8	10	10	15
25	NE	ENE	NW	WNW	5	5	10	15
26	W	W	S	SSW	18	15	5	8
27	SSW	ESE	S	S	8	5	8	8
28	SSW	SW	SW	W	3	14	6	25

February 1974

Date	Air temperature °C 0200	0800	1400	2000	Ice cond. ~0800 E-AM	~1400 E-PM	Water temperature °C 0200	0800	1400	2000
1	-5.0	-6.7	-4.4	-6.1	NONE	NONE	1.7	1.7	1.7	1.7
2	-7.2	-7.8	-3.3	*	ACCR	ACCR	1.7	1.7	1.7	*
3	-1.1	-5.6	-4.4	-4.4	ACCR	ACCR	1.7	1.7	1.7	1.7
4	-6.7	-7.2	-2.8	-7.2	ACCR	ACCR	1.7	1.7	0.6	0.6
5	-10.0	-8.9	-8.9	-7.8	STAT	STAT	0.6	0.6	0.6	0.6
6	-8.9	-10.6	-7.8	-8.3	STAT	STAT	0.6	0.6	0.6	0.6
7	-7.8	-8.3	-2.8	-7.8	ACCR	STAT	0.6	0.6	0.6	0.6
8	-9.4	-10.0	1.7	*	STAT	ACCR	0.6	0.6	1.1	*
9	-6.1	-4.4	3.3	-3.3	ACCR	ACCR	1.1	1.1	1.1	1.1
10	-9.4	-7.8	-2.2	-4.4	ACCR	ACCR	1.1	1.1	1.1	1.1
11	-7.8	*	-5.6	-2.2	ACCR	ACCR	1.1	*	1.1	1.1
12	-1.1	-2.2	6.7	2.2	B-UP	B-UP	1.1	1.1	1.1	1.1
13	1.7	-0.6	0.6	-0.6	STAT	STAT	1.1	1.1	0.6	0.6
14	-3.3	-8.3	-2.2	-6.7	B-UP	B-UP	1.1	1.1	1.1	1.1
15	-9.4	-13.3	-3.9	-4.4	DETR	DETR	1.1	1.1	1.1	1.1
16	-6.7	-5.6	1.1	0.0	ACCR	DETR	1.1	0.6	0.6	0.6
17	-1.1	-2.2	10.0	-1.1	ACCR	ACCR	0.6	0.6	0.6	0.6
18	-1.7	2.8	6.7	4.4	DETR	DETR	0.6	0.6	0.6	0.6
19	5.6	1.7	0.6	-1.1	DETR	B-UP	0.6	0.6	0.6	0.6
20	-2.2	-1.7	3.3	5.6	DETR	DETR	0.6	0.6	0.6	0.6
21	3.3	2.2	7.8	2.2	DETR	DETR	0.6	1.7	1.7	1.7
22	3.3	4.4	-1.1	-3.3	B-UP	ACCR	1.7	1.7	2.2	2.2
23	-5.6	-6.7	-1.7	-6.7	ACCR	ACCR	2.2	2.2	2.2	2.2
24	-8.9	-11.7	-6.7	-7.8	ACCR	DETR	2.2	2.2	1.1	1.1
25	-10.0	-8.9	2.2	-3.3	ACCR	ACCR	1.1	1.1	1.1	1.1
26	-4.4	-4.4	6.7	-1.1	ACCR	*	1.1	1.1	1.1	1.1
27	-1.1	1.1	6.7	5.6	*	*	1.1	1.1	1.1	1.1
28	5.6	4.4	9.4	0.0	*	*	1.1	1.1	1.1	1.1